Proteomic analysis of the Endoplasmic Reticulum of developing castor bean seeds - Testing the feasibility of ER membrane topology elucidation using a sample of purified ER

STOHR, TIM

Tim Stohr

MSc Thesis

Proteomic analysis of the Endoplasmic Reticulum of developing castor bean seeds

Testing the feasibility of ER membrane topology elucidation using a sample of purified ER

School of Biological & Biomedical Sciences

Durham University

Abstract

An Endoplasmic Reticulum (ER) membrane topology elucidation experiment involving ER purified according to Simon et al. [2] was thought to identify yet unknown, tri-ricinoleate biosynthetic enzymes via elucidation of membrane topology and identification of membrane associated proteins. This thesis aims at testing the feasibility of an ER membrane topology elucidation experiment using purified castor bean seed ER prepared according to Simon et al [2].

In a bioinformatics approach, proteins identified in a Multidimensional Protein Identification Technology (MudPIT) experiment of an ER preparation from castor bean seeds were compared to predicted ER localised proteins, thus validating the prediction algorithms, as well as verifying possible contaminations of the ER preparation. Antibodies against identified organelle marker proteins were used in quantitative Western Blot analysis to confirm the degree of purification and contamination. Relative comparison of developing endosperm castor bean ER (dER) preparation with a developing endosperm homogenate showed that, when using anti-oleate Δ 12-hydroxylase (an ER marker protein) antibodies, purification of 58x ER had occurred. When using an anti-VDAC (a mitochondrial marker protein) antibody, a relative quantitation showed that VDAC was 10 x more concentrated in a dER prep than in homogenate. Unlike in previous experiments where mitochondria were purified and 327 mitochondrial proteins were discovered, only 13 could be identified in a MudPIT experiment on *Ricinus communis* ER, thus it can be concluded that mitochondria did not co-purify with dER. The ER preparation was then imaged under a Scanning Electron Microscope. 3 different visualisation techniques were developed to ensure that pictures reflect the original ER preparation state. Vesicles were far more numerous than complex structures. Taking into account the thermodynamics of membranes, it can be said the ER preparation by Simon et al. [2] does not consist of whole ER, but rather ER vesicles.

Contents

List of Illustrations

List of Abbreviations

ER	Endoplasmic Reticulum
MudPIT	Multidimensional Protein Identification Technology
ACCase	Acetyl-CoA Carboxylase
FAS	Fatty Acid Synthase
MCAT	Malonyl-CoA: ACP transacylase
ACP	Acyl carrier protein
KAS	β-ketoacyl synthase
βKR	β-ketoacyl reductase
DH	Dehydratase
ENR	Enoyl reductase
ACS	acyl-CoA synthetase
PC	Phosphatidylcholine
FAD	Fatty acid dehydrogenase
AA	Amino acid
PAP	Phosphatidic acid phosphatase
TAG	Triacylglycerol
DAG	Diacylglycerol
AtPP1	first plant PAP from *Arabidopsis thaliana*
PA	Phosphatidic acid
DGAT	Diacylglycerol acyltransferase
GPAT	glycerol-3-phosphate:acyl-CoA acyltransferase
LPAT	lysophosphatidate acyltransferase
LPA	lysophosphatidic acid
PDAT	phospholipid: diacylglycerol acyltransferase
IMP	Integral membrane protein
MSD	membrane spanning domain
LOPIT	Localisation of Organelle Proteins by Isotope Tagging
PCA	Principal Component Analysis
PLS-DA	Partial Least Square Discriminant Analysis
DAF	Date of flowering
CDP	Critical Point Dryer
TEAB	Triethylammonium Bicarbonate
TCEP	Tris (2-carboxyethylphosphine)
MMTS	Methyl-methane-thiol-sulfonate
IDA	Independent data analysis
3βHSD/D	3-hydroxysteroid dehydrogenase/C-4decarboxylases
VDAC	Voltage-dependent anion channel
MAS	Malate synthase
SEM	Scanning electron microscope
TEM	Transmission electron microscope

1. Introduction

1.1 Background

After cereals, oil crops are the second most important source of calorific intake for humans [6]. However, besides edible uses, they also provide the source for many industrial applications and have the potential to provide many more applications. The problem in their previous low use however was the price. Compared to crude oil, which cost in 1996 about 140 $ per metric ton (http://www.inflationdata.com/inflation/Inflation_Rate/Historical_Oil_Prices_Table.asp), the price of palm oil hovered at around 500$

(http://www.indexmundi.com/commodities/?commodity=palm-oil&months=300).

However in recent years, the prices of crude oil have risen sharply to an average in 2008 of over 500 $ per metric ton (http://www.imf.org/external/np/res/commod/index.asp), increasing the demand for natural oils. Castor bean oil, which can be considered, due to its unusual properties, as a substitute for crude oil, has seen, due to the rising prices of crude oil, a rapid increase in demand. Although castor oil has, for the moment, been mostly a niche product (the reasons for this are explained further in chapter 1.1.1) since it is much more expensive than other vegetable oils, the interest in “green” technologies will ensure a further increase in demand in castor bean oil. The problem here is that increasing the supply of castor bean oil presents some problems due to the difficulty to harvest the oil using conventional methods.

1.1.1 *Ricinus communis* and the agricultural difficulties

The castor bean, *Ricinus communis*, is a perennial shrub that is mainly cultivated in tropical and subtropical areas like India, China and Brazil. Its seed can accumulate up to 60% (w/w) lipids. *Ricinus communis* is a non-determinant plant i.e. the seeds develop at different rates on the same raceme, thereby making optimal harvesting difficult. Furthermore, at the same time the seed produces lipids, it accumulates the very potent toxin ricin as well as the highly allergenic protein albumin 2S. Due to the difference in maturation time of different raceme on the same plant, mechanical harvesting is not possible, thereby endangering the harvesters. Taking into account that *Ricinus communis* only grows in restricted latitudes and that cultivation is, due to the risk involved for the workforce, unthinkable in developed countries, the supply is limited. The difficulties in the cultivation of castor beans and the harvesting of castor bean oil have resulted in prices of about $1000 dollar per ton (http://www.imf.org/external/np/res/commod/index.asp).

1.1.2 *Ricinus communis* and the industrial uses

The oil that can be pressed from the castor bean seeds, castor oil, is special in that it consists of 90% ricinoleic acid. The presence of a midchain hydroxyl group influences the chemical and physical properties of the acid and its esters (Figure 1). This makes it interesting for the industry, which can use it instead of conventional crude oil as starting point for many applications [7].

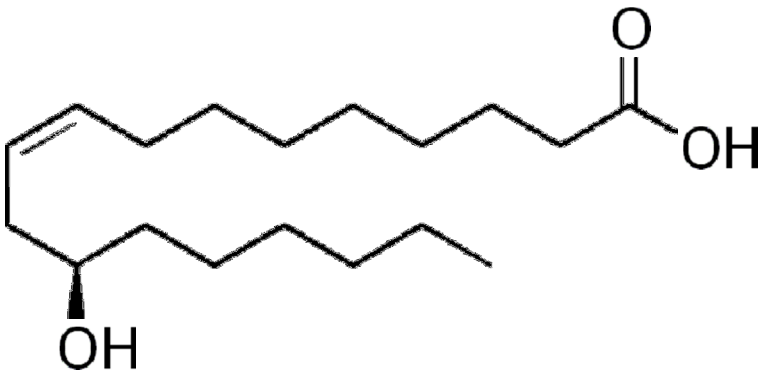

Figure 1: Chemical structure of ricinoleic acid, the major component of castor oil. The hydroxyl group gives the fatty acid its special chemical and physical characteristics.

The different uses of castor oils are described below to emphasize the importance of this oil and the potential gains that could be achieved by increasing the supply of it.

1.1.2.1 Sulfation

By reacting castor oil with sulfuric acid and sulfur trioxide, it is possible to produce a sulfation of the hydroxyl group and a further modification of the double bond. This gives a product with improved surfactant properties. It is used in textile processing, inks, industrial detergents, leather treatment and in lubricative additives for cutting hydraulic fluids and oils [7].

1.1.2.2 Atmospheric oxidation

Castor oil, which has a free hydroxyl group, oxidizes more readily when heated with air than other highly unsaturated vegetable oils. Oils of different viscosities are produced depending on the reaction condition and they have different uses. These oils are used extensively in nitrocellulose lacquers [7].

1.1.2.3 Dehydration

Dehydration of castor oils converts castor oil to a mixture of diene esters and acids that are partly conjugated. These are used as alternative to drying oils such as tung oils. Dehydrated castor oil is used in paints and coating in non-aqueous and recent aqueous formulations. [7].

1.1.2.4 Hydrogenation

Hydrogenated castor oils have higher melting points than the non-hydrogenated materials. Due to the excellent skin-compatibility, these are also used to in the cosmetics industry as well as in paints, coatings and greases [7].

1.1.2.5 Reactions with Ethylene oxide and propylene oxide

Reaction of the hydroxyl group of castor oil with ethylene or propylene oxide gives a nonionic surfactant. By adjusting the reaction parameters, it is possible to obtain oils with different hydrophobicity. The high price of castor oil has hindered the development of this sector. A lowering of the price for castor oil would develop this market. [8]

1.1.2.6 Reactions with isocyanates

Like other hydroxyl-containing molecules, castor oil can be reacted with appropriate isocyanides to form polyurethanes. In the developed world, polyurethane is in high demand to protect the wood from water and mould. Polyurethanes made from castor oil have also been used as encapsulating materials as well, especially in the electrical industry. [8]

1.1.2.7 Splitting with Caustic Soda (C_8 and C_{10} products)

Sodium hydroxide splits the C_{18} ricinoleate into a C_{10} and a C_8 molecule. It is possible, by changing the reactions parameters slightly to produce different products out of ricinoleate. These products are used as efficient lubricants at both low and high temperatures and as solvent in paints.

1.1.2.8 Splitting with steam (C_7 and C_{11} products)

With the development of a continuous steam cracking process, the production of the C_7 and C_{11} aldehydes (which are produced when cracking the ricinoleic acid up using steam) and their uses have increased [7] and will continue to do so in the future. C_7/C_{11} compounds can only be obtained easily from castor oil (due to the hydroxyl group in the oil).

1.1.2.8.1 C_7 compounds

These compounds are available as aldehydes, acids and esters. They are used for example as corrosion protection, low temperature polymer softener and low temperature lubricant (used for example in aircrafts)[7].

1.1.2.8.2 C_{11} compounds

Due to the interchangeable end groups of cracked castor oil C_{11} compounds and unusual build-up (one carboxyl group at the end and an unsaturated center), these have a widespread use. They are currently used as additive to silk, as anti-fungal in cosmetics, paints and cutting oils, as anti-smell compound to reduce the smell of animals and in anti-louse shampoos.

The different uses of castor bean oil were listed comprehensively in Table 1. With the increase in the price of crude oil and the knowledge that our reserves in crude oil are limited and will run out in the next 60 years, it is becoming ever more important to increase the supply of castor oil. The next chapter covers the ways in which the problem is currently tried to be tackled. After a short review of the current knowledge in lipid biosynthesis, the aim of this research will be elucidated.

Table 1: The different uses of castor oil in the industry (Table taken from http://www.castoroil.in/reference/report/report.html).

Agriculture Organic fertilizers	Food Surfactants Viscosity Reducing Additives Flavourings Food Packaging	Textile chemicals Textile Finishing materials Dyeing aids Nylon, synthetic fibres & Resins Synthetic detergents Surfactant, Pigment Wetting agent	Paper Flypapers Defoamers Water Proofing additive
Plastics and Rubber Nylon 11 Plastic films Adhesives Synthetic Resins Plasticisers Coupling agents Polyols	Cosmetics and Perfumeries Perfumery products Lipsticks Hair tonics Shampoos Polishes Emulsifier Deodorants	Electronics Polymers for Electronics Polyurethane Insulation materials	Pharmaceuticals Antihelmintic Antidandruff Cathartic Emollient Emulsifiers Encapsulant Expectorant Laxative & purgative surfactant
Paints, Inks and Additives Inks Plasticizers for coatings Varnishes Lacquers Paint strippers Adhesive removers Wetting additives Finishing materials	Lubricants Lubricating grease Aircraft lubricant Jet engine lubricant Racing car lubricant Hydraulic fluids Heavy duty automotive greases Fuel additives Corrosion inhibitors		

1.2 Castor oil: Solutions to the supply problem

Currently, the world supply of castor bean oil is slightly above 500.000 tons. Due to the development of third and second world countries, the demand is growing at a rapid rate. Since the supply cannot grow as fast, the price for castor bean oil rises steeply.

One of the ways of tackling the problem of supply that is currently attempted by a group [9] is to circumvent some of the plants difficulties concerning the high toxicity by finding and replacing or removing genetically the enzymes that are involved in toxin and allergen production. If this approach works, then the problem of the restricted latitudinal growth and the problem of harvesting still remain. An alternative approach would be to determine the enzymes involved in the biosynthesis of tri-ricinoleic acid production and high oil content in seeds. By then transferring these enzymes to a suitable agricultural crop, like Brassica napus, it would be possible to obtain high tri-ricinoleic production without the danger of toxins and allergens (hence remove the safety issues) and would solve at the same time the problem of restricted growth latitudes. At the same time, such a genetic engineering which involves cross-species transformation also poses safety issues. These go far beyond the scope of this thesis and are discussed in [10, 11].

However, in order to achieve the task of genetically engineering Brassica napus, it is important to understand the lipid biosynthetic pathway that is involved in making storage lipid.

1.3 Storage lipid biosynthesis in plants

One of the earliest successful application of biotechnology to agriculture was the manipulation of seed oil composition. Indeed, the first transgenic seed to get approved for unrestrictive commercial cultivation in the USA was a lauric oilseed rape with changed seed oil composition in 1995 [12]. Two reasons existed for this. First, Brassica napus proved to be a species relatively amenable to transformation, while other cultivated species were more recalcitrant. Secondly, the metabolic pathway involved in lipid storage oil biosynthesis seemed relatively straightforward.

However, later setbacks, especially in achieving the high concentration of specific oils in the seed and the discovery of additional enzymes that affect yields in rather unexpected ways, have shattered the simplicity of the task of genetically engineering plants [6, 13]. The complexity of the seed oil biosynthesis pathway (which leads to the bioengineering difficulties) is explained in the next chapters.

Metabolic pathways leading to neutral lipid synthesis, and hydrolysis are similar throughout the plant kingdom [14]. In the following section, literature on the seed oil biosynthesis from the entire plant kingdom will be reviewed, with special interest towards *Ricinus communis*.

1.3.1 Fatty acid biosynthesis

Plants are different from the other kingdoms in their de novo lipid production in that the first steps are carried out in the plastids. It has to be noted that nearly all the fatty acids produced in seeds are used as storage lipids [6]. The first step of the de novo lipid synthesis requires the enzymes acetyl-CoA Carboxylase (ACCase) and fatty acid synthase (FAS) to work in a concerted fashion. ACCase catalyses the carboxylation of acetyl-CoA to malonyl-CoA using ATP and bicarbonate.

ACCase is the main regulatory enzyme in the lipid pathway and its regulation determine the levels of fatty acid [15].

FAS can be found in two different arrangements in biology. Type I FAS is a very large multi-domain enzyme which is common to mammals, fungi and some bacteria. Each of these domains has a different catalytic site which catalyses a different step of the lipid synthetic pathway [16]. On the other hand, plants and many bacteria (as well as E.coli) have a type II FAS, consisting of 8 different and easily separable enzyme components. These are collectively called FAS II.

After conversion of acetyl CoA to malonyl CoA by ACCase, it can enter the FAS cycle. Malonyl-CoA:ACP transacylase (MCAT) converts malonyl-CoA to malonyl acyl carrier protein (ACP), which is the donor molecule for chain elongation [17].

The elongation begins with the condensation of malonyl ACP with a molecule of acyl CoA catalysed by the enzyme β-ketoacyl synthase (KAS) III. This forms β-ketoacyl ACP, which is then reduced by β-ketoacyl ACP-reductase (βKR) with NADPH as the reductant to give β-hydroxyacyl-ACP. This compound then has a water molecule removed by β-ketohydroxyacyl-ACP dehydrase (DH) resulting in the formation of trans-2-enoyl acyl-ACP. This is then reduced by enoyl reductase (ENR) using NADPH as reductant. The initial sequence of reactions produces butyryl ACP. This 4 carbon compound can then replace malonyl ACP for further elongation of the lipid molecule. However, another enzyme than KAS III is needed in order to perform this: KAS I. Unlike KAS III, KAS I uses acyl ACP (instead of acetyl CoA). By continuing to feed elongated acyl ACPs into the reduction/dehydration/reduction pathway, the acyl chain length increases until it reaches 16 (16:0) of palmitoyl ACP.

Another KAS enzyme called KAS Type II, can then elongate the palmitoyl ACP by a further 2 carbons to stearoyl ACP (18:0). The specific activity of KAS II is important in that it determines the ratio of 16:0 to 18:0 fatty acid molecules leaving the plastid, which in turn influences the degree of desaturation [18]. This whole pathway is summarized in Table 2.

Table 2: Enzymes of plant Type II FAS. After transformation of malonyl-CoA to malonyl ACP, reactions occur in a cycle of condensation, reduction, dehydration and reduction. Three types of KAS enzymes are needed to create 18:0 fatty acids. KASIII initially condenses malonyl-CoA to acetyl CoA. KAS I feeds 4:0 to 14:0 acyl ACP into the cycle. KAS II is needed for the final step which is involved in the elongation of palmitoyl ACP into steroyl ACP (table taken from [19]).

Reaction type	Enzyme name	Short hand	Substrate	Product
Transacylation	Malonyl-CoA:ACP transacylase	MCAT	Malonyl CoA	Malonyl ACP
Condensation (Initial)	β-ketoacyl-ACP synthase III	KAS III	Malonyl ACP (C2) + acetyl CoA	β-ketoacyl-ACP
Reduction	β-ketoacyl-ACP reductase [a]	βKR	β-ketoacyl-ACP	β-hydroxyacyl-ACP
Dehydration	β-ketohydroxyacyl-ACP dehydrase [c]	DH	β-hydroxyacyl-ACP	Trans-2 enoyl acyl ACP
Reduction	Enoyl reductase [b]	ENR	Trans-2 enoyl acyl ACP	Butyryl ACP (C4:0)
Condensation (2^{nd} to penultimate)	β-ketoacyl-ACP synthase I	KAS I	C4:0→C14:0 ACP + acetyl CoA	β-ketoacyl-ACP (C6:0→C16:0)
Condensation (final)	β-ketoacyl-ACP synthase II	KAS II	Palmitoyl (C16:0) ACP + acetyl CoA	β-ketoacyl-ACP (C18:0)

[a] NADPH dependent, [b] NADH dependent, [c] Releases H_2O molecule

The ACPs synthesized in the plastid can go down two pathways. Either they are incorporated into glycerolipids, like monogalactosyldiacylglycerol by acyl transferases or they can be hydrolysed by acyl-ACP thioesterases to produce free fatty acids and ACP. The free fatty acids are then exported out of the plastid. The exact mechanism is not yet determined but the discussions around this subject go beyond the scope of this thesis [20, 21].

The substrate specificity of thioesterases critically influences the pattern of fatty acids which are eventually incorporated into storage triacylglycerol (TAG). Hellyer et al. determined in 1992 the substrate specificity of acyl ACO thioesterases of Brassica napus. They found that the thioesterases had considerable preference for 18:1, which explained the small amount of 16:0 fatty acids exported from the plastid [22].

1.3.2 Fatty acid modifications

Desaturation is the introduction of a carbon double bond into a fatty acid carbon chain. Considering that plant oils are rich in unsaturated fatty acids like oleic (18:1) and linoleic acid (18:2), plants need to have efficient desaturating capacities.

A highly active stearoyl-ACP is present in the plastid stroma which introduces a double bond between carbon 9 and 10 of the fatty acid. This highly active desaturase, which is structurally unrelated to animal or fungi homologs, results in oleate being the main product of exported fatty acids from the plastid[23]. In a bioengineering experiment, this sequence of this enzyme was manipulated in order to reduce the activity of the enzyme. This had a significant impact on the ratio of saturated to unsaturated fatty acids in the oil of Brassica napus [3].

The next set of modification occurs in the ER for plants. Oleate is exported from the plastid to the cytoplasm where it is activated by CoA by the enzyme acyl-CoA synthetase (ACS). The acyl-CoA

molecules are then incorporated into phosphatidylcholine (PC). This is then a suitable substrate for ER-resident desaturases. For example, oleate can then be desaturased further by Fatty Acid Desaturase 2 (FAD 2) to lineoleate (C18:$2^{\Delta 12}$) (where Δ indicates the carbon that has got a double bond) and then to linolenate (C18:$2^{\Delta 12,\ \Delta 115}$) by FAD 3. Although some FAD 2 and FAD 3 plastidial enzymes have been found, experimental evidence suggests that these are mainly involved in the production of specialized thylakoid membrane lipids [24].

The *Ricinus communis* oleate-Δ12 hydroxylase is a membrane bound enzyme that catalyses the hydroxylation of oleate to ricinoleate (18:1-OH). Studies in vivo have demonstrated that this happens via direct hydroxyl substitution instead of proceeding by an intermediate formation of a double bond [25]. Hydroxylase was found to be localised to the ER in 1966. This was confirmed in 2002 by Maltman et al [26] using a purified ER fraction. Using a microsomal preparation of developing castor beans, Bafor et al. showed that hydroxylase only hydroxylates the fatty acids when esterified to PC [27]. It could be shown that the transfer of oleate from labeled oleoyl-CoA to PC was catalysed in the microsomal fraction. . When adding NADH, the radiolabel could be found in ricinoleate which was recovered in the PC fraction or as free fatty acid, thereby indicating that the oleate was catalysed to ricinoleate.

The addition of unlabelled ricinoleoyl-CoA did not increase the low [14C]ricinoleate concentration found in the acyl-CoA fraction nor did it decrease the [14C]ricinoleate concentration found in the PC or free fatty acid fraction. The addition of NADH, which activated phospholipase A to cleave the ricinoleic acid but not the oleic acid from the PC, increased the radiolabelled ricinoleate. Hence, it was demonstrated that hydroxylase will only hydroxylate oleate when it is attached to PC. It could be shown that only oleate that was positioned in the sn-2 position of the PC, however not in the sp-1 position, was hydroxylated. The group also reported that upon addition of Mg_2, ATP and CoA, the ricinoleate released from PC was activated to ricinoleoyl-CoA, which was then readily

incorporated into triacylglycerol by an acyl-CoA dependent acyltransferase [27, 28]. Further evidence that oleate-Δ12 hydroxylase is the enzyme responsible for the production of ricinoleic acid was found in 1995 by Van de Loo et al. [29]. The group proposed the hypothesis that oleate-12Δ hydroxylases (which had evolved independently in several unrelated plant species) may have evolved from a desaturase. Using a cDNA library of castor bean developing seeds, two clones were found that had significant similarity to Arabidopsis ω-3 linoleate desaturase. AA sequence comparison then showed that one of the clones identified had a similarity of 67% to the castor bean FAD2 12-oleate desaturase. Using northern blotting, they were able to prove that indeed hydroxylase was absent from castor bean leaves (which do not produce storage lipids), however present in large quantities in developing seeds (which produces large quantities of ricinoleate) [29].

Using the determined AA sequence, Broun et al. were able to transfect tobacco lines with the putative gene for hydroxylase. These did show a content of 0.1% ricinoleic acid, thereby proving that indeed the gene indentified is responsible for the production of ricinoleate [30].

Some storage lipids have an acyl-chain length greater than C18. These are produced by elongase complexes that are situated in the ER membrane. These use the same reactions as FAS, however use different enzymes. The elongase complex cycles through four successive reactions of condensation, reduction, dehydration and a further reduction [31].

It has to be kept in mind that storage oils do not consist of free fatty acids, since these often have a toxic effect on the cell. Rather, these are stored, using a pathway located in the ER, as TAG. The pathway to the formation of TAG is important to understand since most of the ricinoleate present in the castor bean seed is incorporated into TAG, and the various isoforms of each protein make the task of incorporating the ricinoleate biosynthesis machinery into Arabidopsis challenging.

1.3.3 Phosphatidic acid and Diacylglycerol

Plant energy reserves are not stored in the form of free fatty acids, but rather are esterified to a glycerol backbone to form triacylglycerol (TAG). The chemical properties of TAG molecules make them excellent storage molecules. As they are hydrophobic, they require less water for hydration than polysaccharide (thereby they can pack closer) and can store more energy per gram than any other component of the cell [32].

The fatty acids produced in the plastid are transferred to the ER and esterified to a glycerol backbone. The classic reaction pathway for the biosynthesis of fatty acids is called the Kennedy pathway [33, 34]. It consists of a series of reactions (Figure 2) which sequentially acylate a G3P molecule via the intermediates monoacylglycerol, phosphatidic acid and diacylglycerol. The final step of TAG synthesis however can occur via two different pathways: the Acyl-CoA dependent and Acyl-CoA independent pathway. Both of these will be considered separately in chapter 1.3.4.1 and 1.3.4.2 .

G3P is acylated with 1 acyl-CoA via the action of glycerol-3-phosphate:acyl-CoA acyltransferase (GPAT) at the sn-1 position to create lysophosphatic acid. Although this enzyme long resisted cloning [19], a gene family was successfully cloned in 2003 from Arabidopsis [35]. It was found that seven isoforms of this enzyme exist, with differential expression patterns in different tissues. Until now only GPAT1 and GPAT5 have been studied. GPAT1 was found responsible for the differentiation of the pollen and male fertility [35], and GPAT5 for the production of glycerolipids that act as a pathogen barrier in seeds and young roots. Knock-outs of either of these did not affect the composition or content of storage lipid. Each of the remaining 5 GPAT isoforms could have the specialized function of incorporating a ricinoleate into the G3P backbone in *Ricinus communis*.

The acylation of lysophosphatidic acid (LPA) is catalysed by lysophosphatidate acyltransferase (LPAT) at the sn-2 position of LPA resulting in PA (Figure 2). An early insight into the selectivity of LPAT was revealed in 1984 when Ichihara et al. showed, using safflower microsomes, that saturated fatty acids did not show selectivity to incorporation into either sn-1 or sn-2 position [5], when incubating with unsaturated fatty acids. When incubating only with unsaturated fatty acids, the sn-2 position was rarely occupied. This showed that indeed LPAT had a preference for saturated acids. A study of the selectivity of LPAT in rapeseed showed that no C22:1 was incorporated into the sn-2 position at all [36]. However, in 1995, Brown et al. were able to show that when cloning two LPAT isoforms (one of which was presumed to have a selectivity towards the unsaturated C22:1) from Limnanthes douglasi into Brassica napus, it could be shown that the introduction into sn-2 of C22:1 was increased dramatically [37]. Hence, Brown et al. showed that the selectivity of LPAT is not as clear cut as previously thought by Cao et al. Rather, the selectivity depends on different isoforms of the same enzyme, which also have differential expression patterns.

In 2005, a further complication appeared. Five different LPAT isoforms had been reported to be ER located in Arabidopsis thaliana [38]. Each one of these isoforms could be specialized in *Ricinus communis* to perform the acylation on a LPA containing a ricinoleate. The possibilities of enzyme combination have been drastically increased.

Phosphatidic acid phosphatase (PAP) then removes the phosphate from the sn-3 position of PA and forms diacylglycerol (DAG). Since PA is also the precursor for phosphatidylinositol, phosphatidylserine, phosphatidylethanolamine and phosphatidylglycerol, the relative rate of the enzyme PAP is determinant of which pathway the majority of the PA flows down. PAP was first identified in 1955 [39], but it was only purified to homogeneity in 1998 [40]. It is a 51 kDa protein that shows wide substrate selectivity, not only dephosphorylating PA but also sn-1 LPA, sn-2 LPA

and ceramide-1-phosphate. [40]. In 2001, Pierregues et al. cloned the first plant PAP from Arabidopsis thaliana (AtPP1), and identified it by homology to yeast and mammalian PAP [41]. In this study, another PAP gene could also be identified by homology to AtPP1. However, this gene had different expression patterns and different substrate selectivity when compared to AtPP1.

In 2007, Nakamura [42] identified and cloned 3 different plastidic PAP homologs from Arabidopsis. Although, plastidic PAP are mainly involved in the biosynthesis of membrane lipids, it shows the existence of isoforms of this enzyme. In 2008, França et al. were able to isolate and characterize two different PAP genes from cowpeas. The isoforms locate to some similar organs however show a differential expression patter in seeds, flowers and roots. One of them (called VuPAPα) accumulates during seed development, while the other one (VuPAPβ) does not play a role in seed development [43].

Previous experiments involving the bioengineering of Arabidopsis to express high concentration of ricinoleate in its seed have resulted in a maximal 25% seed oil content [44]. The reason for this low accumulation is not understood [44]. However, it may be possible that the incorporation of ricinoleate into TAG in *Ricinus communis* is dependent on an isoform of the Kennedy pathway enzymes that is restricted to castor bean, which would be able to accommodate the stereochemically different ricinoleate. The high numbers of different isoforms, however have been a problem in determining exactly which isoforms would increase the ricinoleate percentage in seed oil content.

In order to achieve the 90% ricinoleate concentration seen in castor bean oil seeds, it is also important to understand the last step of storage lipid production: the integration of a further ricinoleate into DAG.

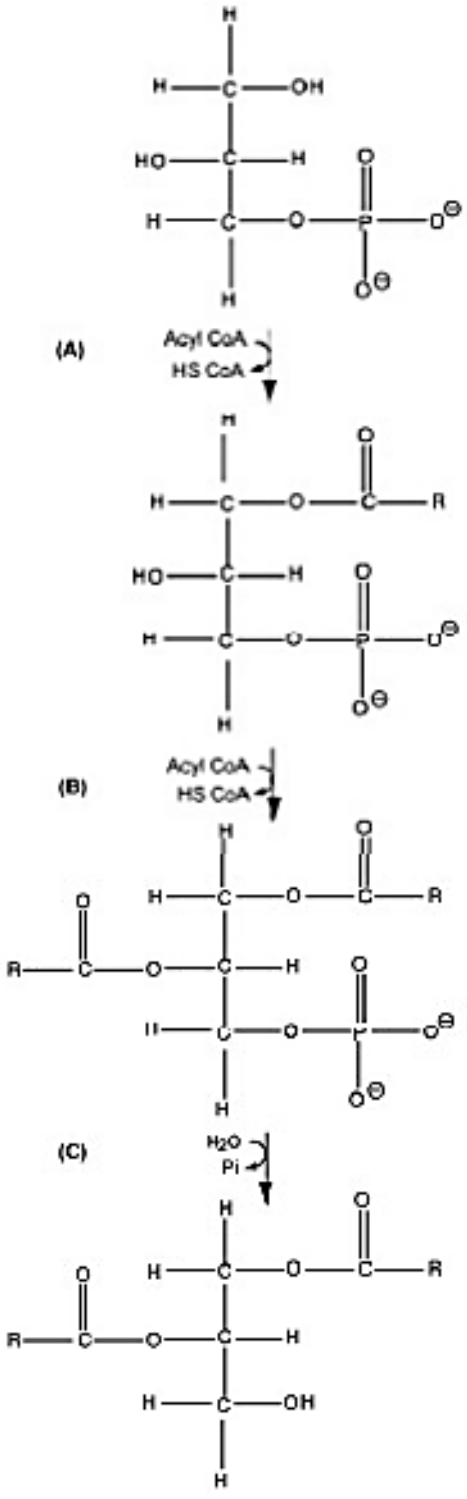

Figure 2: Route of PA and DAG synthesis. G3P is acylated at the sn-1 position by GPAT to form LPA. This molecule is then acylated at the sn-2 position with a further acyl-CoA molecule by LPAT to form PA. Dephosphorylation of PA is then catalysed by PAP to form DAG.

1.3.4 TAG production

The last step in the production of storage lipid is the acylation of the sn-3 position of the DAG to form TAG. This can happen through two different pathways. One involves an acyl attached to CoA as substrate (the CoA dependent pathway) and the other one uses acyl chains that are independent of CoA molecules. The results are the same, a glycerol derived molecule with 3 acyl groups attached to it (Figure 3).

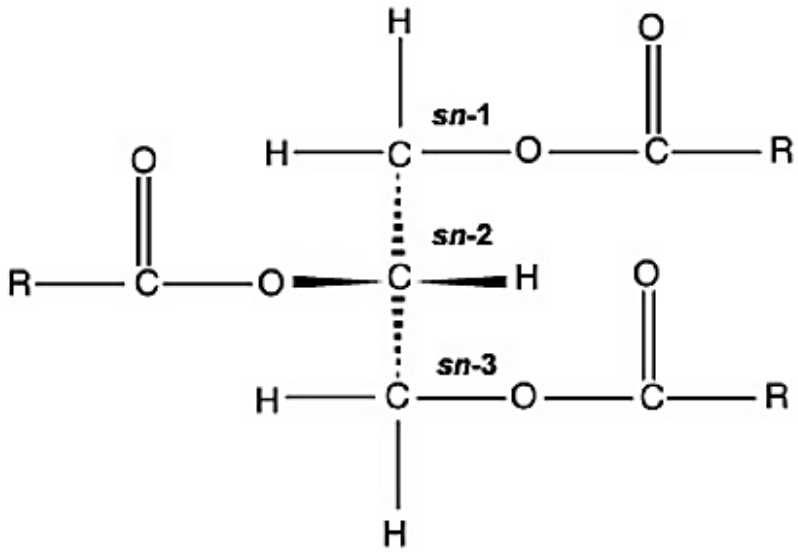

Figure 3: Structure of a TAG molecule. R denotes the acyl side chains. The glycerol backbone is stereochemically active, therefore the carbons can be distinguished. Each carbon has been named sn.

An analysis of the composition of the fatty acids at each of the sn positions in TAG from different oilseeds revealed a significant difference not only between the different oils but also between different TAG (Table 3).

Table 3: Analysis of the position of acyl chains. Heterogeneity of position can be seen not only between different plant species but also between different plant varieties. [19][19] [16]

		Fatty acids (%)						
Species	*sn* Position	16:0	18:0	18:1	18:2	18:3	20:1	22:1
B. napus (Rape) high erucic acid [a]	1	4	2	23	11	6	16	35
	2	1	0	37	36	20	2	4
	3	4	3	17	4	3	17	51
B. napus (Rape) low erucic acid [b]	1	6	2	65	16	7	2	1
	2	Trace	Trace	53	31	16	Trace	Trace
	3	8	2	71	10	5	3	1
Glycine max (Soya) [c]	1	14	6	23	48	9	-	-
	2	1	Trace	22	70	7	-	-
	3	13	6	28	45	8	-	-
C. tinctorius (Safflower) [d]	1	9	2	8	81	-	-	-
	2	0	0	8	92	-	-	-
	3	4	1	7	88	-	-	-

[a] Brokerhoff et al. [1] [b] Knutzon et al.[3] [c] Gunstone et al.[4] [d] Ichihara et al.[5]

Dahlqvist et al. demonstrated in 2000 [45] the difference in selectivity of the enzymes that catalyse the DAG to TAG reaction, even though the plants used the same pathway. It could be shown that the enzyme responsible for the acyl-CoA independent pathway (phospholipid:diacylglycerol acyltransferase) showed preference for vernoloyl groups in Crepis paleastina, while in castor bean it preferred both ricinoleoyl and vernoloyl. This difference in selectivity can also be seen in the above table (Table 3). For example, the high erucic acid variety of Rape has 51% C22:1 in the sn-3 position, while the low erucic acid variety only has traces of it. Furthermore, little selectivity exists as well as to the acyls that occupy sn-1 and -2. Taking again the example of high and low erucic acid rape variety, the compositions of the sn-2 position is different between both. 18:1 gets incorporated between 53 and 71% of the time in any position in the low erucic acid variety with sn-2 being the lowest, while in the high erucic acid variety 18:1 gets incorporated at a rate between 4 and 36 where the sn-2 position is the highest scoring.

1.3.4.1 Acyl-CoA dependent pathway

Diacylglycerol acyltransferase (DGAT) is responsible for the last step in TAG formation, acylating DAG to TAG. It has previously been cloned from several organisms including Arabidopsis thaliana [46] and *Ricinus communis* [47]. An experiment involving the overexpression of DGAT showed that the average seed weight and the lipid content increased in relation to the amount of DGAT present [48]. Further evidence suggests that although alternative routes from DAG to TAG exist, these are not quantitatively significant in seed oil biosynthesis in Arabidopsis thaliana, oil olive and oil palms [49-51].

In 2001, a further DGAT gene family was identified in Mortierella rammaniana [52] named DGAT2 and subsequently also characterized in mice [53]. Following an investigation into the ricinus oil synthesizing machinery, Kroon et al [54] were able to clone the gene for DGAT2 of *Ricinus communis* as well as to determine the expression pattern. It was found that DGAT2 is 18x higher expressed in the developing seeds than in leaf and that the expression is temporarily limited [54]. This result was confirmed in 2006 by Shockey et al. who cloned DGAT2 from tung tree and also found that DGAT2 is the biochemically significant protein in oil biosynthesis in developing seeds [55]. Interestingly, they also found that DGAT1 and DGAT2 localise to different parts of the ER, which strengthens the theory of subdomains. It is thought that the high concentration of ricinoleate in castor bean oil is achieved via metabolic channeling. The current theory is that the ER is composed of subdomains which consist of enzymes of one pathway localising to one part of the ER and then working in conjunction to produce the high concentration of ricinoleate seen in the seed oil. Further evidence which supports the theory of metabolic channeling is present, however a review of this material goes beyond the scope of this thesis [56].

1.3.4.2 Acyl-CoA independent pathway

In 2000, Fraser et al. deactivated the PAP in sunflower microsomes by the addition of EDTA (which collates Mg^{2+}, a vital co-substrate for PAP). Therefore, PA accumulated. When then washing the membranes in a buffer containing Mg^{2+} (therefore reactivating PAP to catalyse PA to DAG) and incubating either with or without acyl-CoA, no difference in TAG produced between the differently treated samples could be found. It was proposed that other enzymes than the acyl-CoA dependent DGAT are responsible for producing TAG. They also suggested that this route may be quantitatively important for some plants [57]. In the same year, Dahlqvist et al. were able to identify a pathway that is an acyl-CoA independent route that uses PC as acyl-donor and DAG as acceptor [45]. The enzyme phospholipid:diacylglycerol acyltransferase (PDAT) was identified in Helianthus annuus, Crepis palestina and *Ricinus communis* [45].

The PDAT gene was isolated from Arabidopsis thaliana in 2005 [50] by homology to the yeast PDAT. This allowed mutants of Arabidopsis thaliana in PDAT to be identified. It was found that in this organism, PDAT does not contribute to TAG production [49]. The redundancy in the storage lipid production opens the question of the reason for the evolution of this protein. It is thought that PDAT evolved to store away toxic fatty acids from the membrane into storage TAG (ricinoleate is not present in membranes [58]). Considering now the case of castor oil, the indigestibility of the oil will have acted as deterrent for animal predation. Therefore the PDAT enzyme has been highly tuned to the transfer of this unusual fatty acid, giving the plant an evolutionary advantage. Hence, most of the TAG production

In the previous chapters, the current knowledge on storage oil biosynthesis has been presented. This will help to understand and appreciate the aims of this thesis. Furthermore, it will show the

importance of a topological analysis of ER. A short review of the methodology behind a topology elucidation will be presented in the chapter after the aims of the whole group.

1.4 Aim of the whole group

In order to fully understand the importance of the research done in this thesis, it is vital to understand the aims of the group led by Prof Slabas.

As detailed beforehand, bioengineering of crops can bring high economic rewards, especially with respect to the castor bean oil. The plant that produces it is exceptionally toxic and not very well adapted to agriculture. Although some projects are currently ongoing to reduce the toxicity of *Ricinus communis* [65, 67], this approach will not solve the agricultural problem. By transferring the biosynthetic machinery of castor bean oil production into Brassica napus, it would solve both the toxicity problem as well as allow castor oil to be grown in agricultural crops.

The general aim is to identify specific enzymes involved in the synthesis of tri-ricinoleate and following cloning of the genes, to insert them into Brassica napus. In this way, it is hoped that the rape plant will synthesize high levels of triricinoleate without problems arising from toxic and allergenic proteins. Furthermore, it is hoped to prove the theory of heterogeneity of the ER (ie the proteome of the ER consists of metabolic complexes with precise location and arrangements) and membrane channeling in the lipid biosynthesis. Broadly speaking, two methods exist for the determination of gene function. The genetic approach involves the transfer of candidate genes from *Ricinus communis* to Arabidopsis. This approach would not be useful in the current application since no target gene could be identified yet. The other approach, based on proteomics, would be to first identify the proteins involved in the biosynthetic machinery of ricinoleate production, to get the genes responsible and then to transfect plants with these genes. The

castor bean genome has now been completely sequenced, which allows the identification of target genes.

1.5 Methodology of membrane topology in castor bean ER

The aim of proteomics is the identification of all the proteins in an organism, a tissue, a cell or an organelle [59]. A protein can be identified by identifying its unique AA sequence.

Integral membrane proteins (IMPs) pose a bigger problem than soluble proteins. They are embedded in a membrane, therefore have regions which are exposed to 2 or 3 spatially different locations: the lumen, the cytoplasm and the hydrophobic membrane. Although the prediction algorithms of membrane spanning domains (MSD) have advanced to a high level of accuracy [60], it is difficult to predict lumenar or cytosolic sides of IMPs. Determination of membrane topology gives answers to these questions, so represents a strong tool in IMP structural architecture determination.

One of the critical requirements for discovery of membrane topology is to have intact highly purified ER. Considerable research aiming at the isolation and purification of ER membranes of castor beans has been done. An overview of previous methods for ER isolation will be presented, followed by presentation of the ER-isolation method that will be used in the current investigation. However, a criteria for purity needs to be defined. The next part will deal with these issues.

1.5.1 ER isolation

In 1973, Kagawa et al. [61] developed a method for the separation of organelles of germinating castor beans, using a continuous sucrose gradient. 3 bands could be seen, out of which two were identified as the glyoxysome and mitochondria fraction. Lord et al. [62] were then able to show that the unidentified band is composed of the endoplasmic reticulum. Moore et al. [63] confirmed that the unidentified band seen by Kagawa et al. [61] is indeed endoplasmic reticulum.

Coughlan et al [64] used a variation of the protocols developed by the group of Beever [62] for extraction of germinating ER (gER). Instead of a continuous sucrose buffer, Coughlan used a discontinuous buffer, thereby facilitating identification and extraction of the required band, at the cost of lower resolving power of the sucrose buffer.

The endosperm of germinating castor beams were extracted and homogenised in a homogenisation buffer. After low g centrifugation step to separate the fat and the cell detritus from the rest of the homogenate, the homogenate was layered on top of a fraction of 20% sucrose. Below the 20% sucrose was a linear fraction of 60-30% sucrose. It could be shown that the ER fraction collected at the interface of 20-30% sucrose after 2h at 25,000 rpm. The protein band was then collected by piercing the centrifugation tube with a needle. About 3 ml of the solution containing the crude ER were then mixed with a saturated sucrose solution to obtain a solution of ~50% sucrose. This was then placed in the bottom of an ultracentrifuge tube, and overlaid by a solution of 40%, 30% and 20% sucrose solution respectively. This was then centrifuged at 25,000 rpm for 24h. The purified ER was then collected at the interface of the 20-30% sucrose gradient, again by piercing the centrifugation tube with a needle. The purified ER was then isolated and mixed with ice-cold distilled water. The membranes were then pelleted by

ultracentrifugation at 55,000 rpm. The pellet was then resuspended in distilled water and stored at -80°C.

It is important to collect intact ER membrane compartments. In order to do achieve this, it is important to exert the least possible sheering force on the sample. This is why the time-consuming but gentle homogenisation with a razor blade is preferred over homogenisation with a blender. The isolation via sucrose gradient is also designed to reduce sheer force. Using this technique, in comparison to differential centrifugation described in [62], the ER compartment is isolated via its unique density in a double sucrose gradient, rather than by pelleting. For the siphoning off of the white band of ER after the first purification step, a big needle is used to reduce sheering forces exerted on the collected ER. Furthermore, when pooling the samples, the needle is taken off the syringe when transferring the content of the syringe into the pooling container [2, 63].

The other important factor in elucidating membrane topology is purity. When determining membrane topology, the ideal case would be to possess a completely pure sample of ER membrane compartment. However, during homogenisation membrane compartments burst open. One explanation may be that, although homogenisation with a razor blade is lot more gentle than homogenisation with a blender, the sheer forces exerted using the razor blade are strong enough to break some membranes. Proteins that resided in spatially different location can therefore interact. Some of these proteins will have intrinsic affinity for the cytosolic domains of ER IMPs or for the ER lipid membrane, especially since the ER produces the phospholipids that are present in all other membranes. Therefore these proteins could be co-isolated as contamination with the ER compartment. These contaminations will only be present in the cytosolic part of the ER.

Furthermore, as was described in a paper by Dunkley et al [65], it is very difficult to obtain pure organelles. To show this, Dunkley et al. used a linear self-generating iodixanol gradient. Iodixanol gradient is similar to a sucrose gradient apart from that the linear gradient forms from a homogenous solution when centrifuged at high-speed for a few hours. These gradients are highly reproducible because their shape only depends on the starting concentration of ioxidanol and the centrifugation time[66]. Traditionally, organelles are assigned a localisation on this gradient according to their density. Their position is confirmed by western blot, staining for marker proteins of the organelles with adjacent position in the gradient. However, Dunkley et al were able to determine several different contaminants from other organelles than just the adjacent.

In order to quantify the amount of contamination, Dunkley et al. developed a technique called Localisation of Organelle Proteins by Isotope Tagging (LOPIT). It allows analysis of protein distribution across the gradient rather than the cataloguing of single fractions.

The workflow of LOPIT has been described in Figure 4. The organelles of a sample, in this case from an Arabidopsis callus, were partially separated on a linear self-generating ioxidanol gradient. To determine the distribution of ER and Golgi, gradient fractions were analysed using Western Blot with antibodies against the Golgi marker protein gtl-6 and the ER marker protein AtSec12. It could be shown that the gradient only partially separated the organelles. Analysis using LC-MS/MS showed several proteins of other organelles being present at the same place in the gradient as the Golgi, clearly showing that it is not possible to purify completely an organelle, although it has to be said that the specific organelle concentration is increased at respective localisations along the gradient. Thus it is necessary to analyse to what extent a sample is contaminated.

To determine the distribution of organelles along the gradient, Dunkley et al. used the cleavable ICAT reagent to allow relative quantification. In total six pair-wise comparisons were done. The proteins of each sample were labelled with an ICAT reagent: the light fraction with the light ICAT

reagent and the dense fraction with the heavy ICAT. The two fractions were then pooled, separated using an avidin-affinity column and analysed using LC-MS/MS. 13 of the 170 proteins identified had been localised to a specific organelle beforehand and 15 could be localised to specific subcellular location based on homology with proteins from other plants and animals or yeast. Using Principal Component Analysis (PCA) and Partial Least Square Discriminant Analysis (PLS-DA), and the known localisation of the 28 above described proteins, Dunkley et al. were able to confirm their LOPIT technique for the identification of contaminant proteins and organelles in a purified organelle solution. Furthermore, they report this technique as being able to localise previously unknown proteins to an organelle.

This methodology has been updated to use the more versatile iTRAQ 4plex reagent instead of the ICAT reagent. However, the overall strategy does not change due to the change in labelling reagent [67].

Dunkley et al. then present the data obtained using the LOPIT approach for the localisation of some proteins to the organelle which they co-elute with, however, since an *Arabidopsis* callus suspension culture was used which does not produce any lipids, no lipid producing enzymes should be present. Since the focus of the elucidation of membrane topology is the identification of complexes involved in lipid production, this experiment is only relevant to the extent of pointing out the fact that obtaining pure samples is not possible and identification of peptides not belonging to the ER could be identified in ER samples. The concentration of ER will be determined using Western blotting and antibody fluorescence (Chapter 3.2), a qualitative determination of the contaminants done using a bioinformatics approach (Chapter 3.1) and a qualitative assessment of the contamination using antibodies fulfilled in Chapter 3.2.

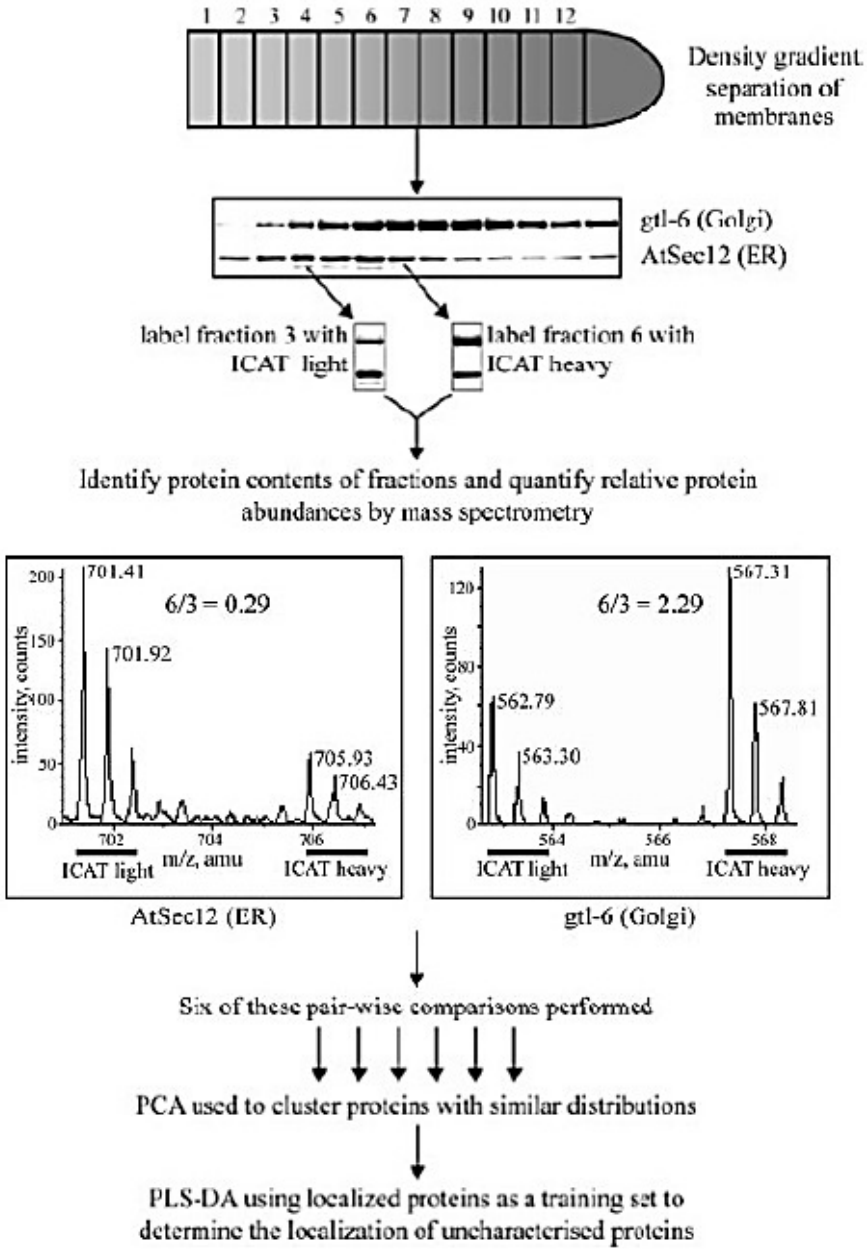

Figure 4: LOPIT workflow. Organelles from a sample, in this case Arabidopsis, were separated using a linear self-generating ioxidanol gradient. Golgi and ER organelle-distribution were determined by Western blot with an antibody for the Golgi apparatus marker gtl-6 and the ER marker AtSec12. Protein distributions were determined by performing six pair-wise comparisons across the gradient. The lighter fraction was labeled with ICAT light and the heavy fraction with ICAT heavy. The labeled peptides were then pooled, digested and avidin-affinity filtered. The ICAT labeled peptides were then analysed using LC-MS/MS. Proteins were assigned to organelles by matching their distributions to those of proteins that have known subcellular localisation. To do this, two method of analysis are used: PCA and PLS-DA. Figure taken from [65]

Dunkley et al. [67] raise an important issue that will affect the elucidation of membrane topology of ER of developing and germinating castor beans. It is not possible to obtain totally pure ER. The reason for this is that organelle separation using gradients is not efficient, as demonstrated by Dunkley et al. [65], and proteins from other organelles may have affinity for ER IMPs. The latter problem can be solved by washing the isolated ER with a KCl solution and/or mild detergent to rid the IMPs of proteins attached by ionic or hydrophobic affinity. However, one of the reasons for the importance of elucidating membrane topology is the determination of proteins that interact with known storage lipid producing enzymes, which would also be washed away by the salt wash or the detergent. This problem can only be circumvented by identification of the contaminant proteins. However, identification of contaminant protein is difficult because previous experiment may have assigned the contaminant to a wrong localisation, hence these will be classified wrongly in databases. Therefore critical appraisal of the literature is important when determining which proteins are contaminants and which are interacting in vivo with protein in the ER. Another way to circumvent the problem of contamination is to determine the level of contamination and use it to indicate the confidence that can be put into the data. However, this method is difficult since it would involve the quantification of each contaminant protein, and identification of all contaminating proteins is difficult. More research that would breach the scope of this MSc thesis is needed in order to exactly quantify the contamination of the ER preparation by Simon et al [2].

A problem for the identification of ER IMP associated proteins pose the proteins requiring posttranslational modification to localise to the ER. These are only interacting with the ER when post-translationally modified; therefore these can also be considered as contaminant. Identification of these proteins as contaminants is difficult. An in vivo study to identify the localisation of each interacting protein in vivo needs to be done in order to identify these proteins. However, this lies beyond the reach of this literature review.

In order to determine membrane topology, a method for the differentiation of the luminal and cytosolic domains is needed. Proteolysis of the outer surface of the ER would reveal which proteins are on the outside. Clearly, if the ER is not intact, the results would be compromised. The use of protease protection strategies is critical to understanding ER topology. The complications involved in such analysis, as well as the pre-requirements are discussed below.

1.5.2 Protease protection assays

Protease protection assays are standard methods used in the determination of the membrane topology [68-70]. This method has been used elegantly by Wu et al. [71] when working on elucidation of membrane topology in rat brain Golgi.

Protease protection can be divided in three steps (Figure 5). The first step usually involves digestion of the extralumenar proteins by a protease (step 1). The lumenar proteins and the lumenar domains of proteins are protected from the protease by the membrane. The shaved off peptides are then detected and analysed in a MS/MS apparatus.

The membrane compartment is then re-isolated (step 2). Upon addition of detergents the membrane is disrupted and the lumenar proteins and the lumenar domains (and the hydrophobic domains) of the IMPs, which have been previously protected by the membrane from the protease, are digested using a protease (step 3). Analysis and sequencing with a mass spectrometer allow the identification of the lumenar domains [71].

In order to understand the pre-requirements that membrane topology elucidation has, it is important to understand the methodology that is used. Figure 5 shows the critical steps involved in a protease protection strategy and points out the need to have intact membrane compartments.

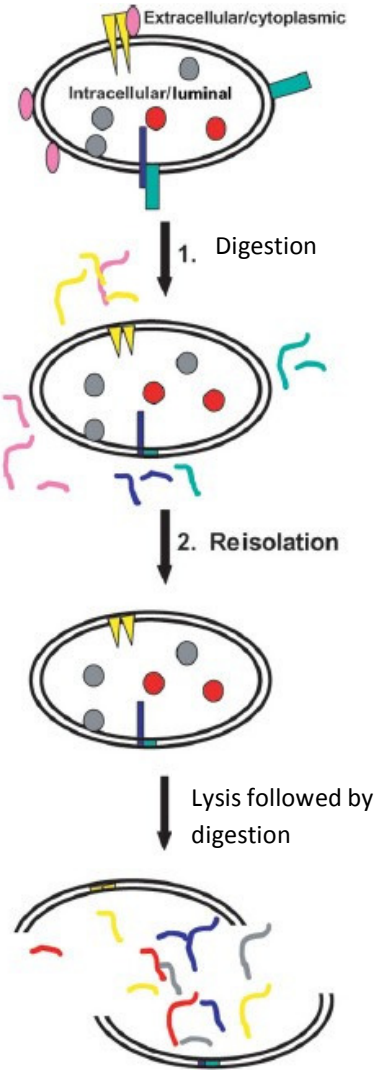

Figure 5: Schematic showing a protease protection strategy. Using a protease protection protocol, the method can be separated into sequential steps, allowing membrane topology analysis and protein localisation. The extralumenar proteins are cleaved with proteinase K. After re-isolation of the membrane compartment, high pH is used to form membrane sheets. Proteinase K is then used to cleave the lumenar proteins and lumenar domains. Subsequent identification allows identification of sidedness of proteins. Picture taken from [72]. As can be seen, this method relies on the wholeness of the membrane compartment (membrane compartments that have been split once will not have cytosolic proteins anymore)

1.5.3 MudPIT experiment of ER from developing castor bean seeds

Simon et al. (unpublished data), isolated three samples of ER from developing *Ricinus communis* seeds, as well as three samples of ER from germinating seeds using the method described by Simon et al.[2]. However, instead of storing them in glycerol, the pellets were re-dissolved in 2D lysis buffer (9 M Urea, 2 M thio-urea, 4 % CHAPS). They then were acetone precipitated, acetone washed, re-suspended in a small quantity of triethylammonium bicarbonate (TEAB) and quantified using a Bradford Protein Assay (Bio-Rad Laboratories Ltd).

A total of 100 µg of each protein sample was reduced in tris(2-carboxyethylphosphine) (TCEP), alkylated using methyl-methane-thiol-sulfonate (MMTS) and digested with trypsin overnight at 37C. Tryptic digests were dried, re-suspended in TEAB (pH8.5) and labeled with iTRAQ reagents (Applied Biosystems) for 1 hour at room temperature. Labeled peptides were then mixed to generate a pooled sample containing each of the four iTRAQ tags.

The pooled sample was vacuum dried and re-suspended in 2.0ml 10mM K_2HPO_4 / 25% acetonitrile, pH 2.8 strong cation exchange (SCIEX) buffer. The complexity of the digest mixture was reduced offline by fractionation on a Poly-LC (200x2.1mm) SCIEX column to give 25 fractions for subsequent LC-MS–MS analyses.

The fractions were vacuum dried and then resuspended in 90ml of 2% acetonitrile 0.1% formic acid. 30 ml of each fraction was analysed by LC-MS/MS using a nano-flow Ettan MDLC system (GE Healthcare) coupled to a hybrid quadrapole-TOF mass spectrometer (QStar Pulsar i, Applied Biosystems) fitted with a nanospray source (Protana) and a PicoTip silica emitter (New Objective).

Each sample was loaded and washed on a Zorbax 300SB-C18, 5mm, 5 x 0.3mm trap column (Agilent) and online chromatographic separation was achieved over 2 hours on a Zorbax

300SB-C18 capillary column (3.5 x 75µm) with a linear gradient of 0-40% acetonitrile, 0.1% formic acid at a flow rate of 200nl/minute.

MS data were acquired using the Independent Data Analysis (IDA) component of Applied Biosystems Analyst software version 1.1 switching between survey scan and 3 product ion scans every 10 seconds. Only ions with 2^+ to 4^+ charge state and with TIC > 10 counts were selected for fragmentation.

All MS/MS data files were processed using ProQuant software version 1.1 (Applied Biosystems, USA) using the JCVI Tigr castor bean database for *Ricinus communis* sequences. MS and MS/MS tolerances were set to 0.15 and 0.1 Da respectively and cleavage sites were defined as lysine and arginine with a single missed cleavage, MMTS cysteine, oxidised methionine, iTRAQ –Lys and iTRAQ- Tyr modifications allowed for in the database search.

In order to reduce protein redundancy, and determine protein identification confidence scores (ProtScores) and quantification statistics from the ProQuant output for each fraction, the data from all fractions were combined, analysed and reported using ProGroup software (Applied Biosystems). Proteins that were identified as always present in each biological replicate were assembled into a single table and average ratios and standard deviations calculated for each protein. Differentially expressed proteins were defined as those with a fold-change greater than 1.2 that was significant in each replicate ($p \leq 0.05$)

This experiment was then repeated, except that 0.2% SDS was added to the TBA re-suspension.

It has to be noted that the author was not involved in performing this experiment.

1.6 Aim of this thesis

The aims of this thesis are:

1. Compare proteomics data from Dunkley et al. [65, 67] to *Ricinus communis* ER MudPIT data from

   Simon et al. (unpublished data)

   a. Identify target genes that encode known activities in storage lipds synthesis but are *Ricinus communis* specific isoforms that can increase the yield when cloned into Arabidopsis thaliana.

   b. Identify the nature of the protein contamination in a standard ER prep as prepared according to Simon et al. [2] (qualitative contaminant analysis).

2. Quantify

   a. The amount of purification of ER using an ER marker as compared to an endosperm homogenate.

   b. The amount of mitochondrial contamination, as indicated by a mitochondrial marker, in a standard ER preparation as compared to an endosperm homogenization (quantitative contaminant analysis)

3. Determine the intactness of a standard ER preparation by using scanning electron Microscopy by comparing it to the only available SEM picture of ER.

4. Determine if the pre-requirements of intactness of ER and acceptable levels of contamination are met for an ER membrane topology experiment.

2. Method

2.1 Plant germination

Ricinus communis plants (batch number 99N89) were germinated by incubating for 24 hours in a Buchner flask under constant water flow. 6 seeds were transferred to a large plastic beaker (3 litre volume), filled with vermiculite. Care has to be taken that the vermiculite is soaked in water and 5 centimeters of the bottom of the beaker are filled with water. The seeds were then covered with a small amount of wet vermiculite. The beaker was covered with plastic film to prevent dessication and left to incubate at 30°C in the dark for 2 days. The germinated seeds with the beaker are then transferred to the growth chamber.

2.2 Plant growth

The plants were grown in a Fitotron (Fitotron® SGR "Walk in"). They received 16 hours light per day. The temperature was kept at a constant 26°C during daylight time and at 22°C in the dark. The humidity was not controlled for. The soil in the plants pots were kept humid and watered every day. The soil composition was a 60 to 40 % mixture of flower compost and sand. Plant feed was given to every flowering plant once per week. The Date of Flowering (DAF) was determined as the date when 8 flowers could be seen on a raceme.

2.3 ER preparation from developing castor beans

Developing castor bean seeds were harvested at 25 days after DAF. The seeds of 2 racemes were then cut in half and the endosperm removed using a small spatula and placed in an ice-cool glass plate with 40 ml homogenisation buffer (500 mM sucrose, 10 mM KCl, 1 mM EDTA, 1 mM MgCl, 2mM DTT, 150 mM Tricine/KOH pH7.5, 0.1 mM PMSF). The method of Simon et al. [1] was then used to prepare the ER.

2.5 1-D Mini gel

The gels were cast using the Mini protean II gel casting set from Bio-Rad Laboratories (Bio-Rad Laboratories Ltd.).

2.5.1 Gel casting

1-D gels were routinely used as a 12% acrylamide gel. These were cast using the Mini protean II (Bio-Rad Laboratories Ltd.) gel casting set with 0.75 mm thickness and clean glass plates. The gels were cast using 12% acrylamide (acrylamide:bis-acrylamide 37.5:1), 375 mM Tris-HCl pH 8.8, 0.1% (w/v) SDS, 0.05% (w/v) ammonium persulphate, 0.2% (v/v) TEMED. The solution was then cast in between the clean casting plates and overlaid with water saturated butan-1-ol. When the gel had set, the butan-1-ol was removed and the plates were rinsed with purified water. The stacking gel was then similarly cast, only using 5% acrylamide and 125 mM Tris-HCl pH 6.8 as buffer, on top of the resolution gel.

2.5.2 Sample preparation and gel loading

Unless otherwise indicated, 8 µg of sample at a concentration of 1 mg/ml were solubilised in 2 µl of 5 x SDS sample buffer (10% (w/v) SDS, 5% (w/v) DTT, 0.05% (w/v) bromophenol blue, 0.312M Tris-HCl pH 6.8, 50% (v/v) glycerol) to give a 1x concentration in a volume of 10µl. If the starting solution was too dilute, the total volume was raised up to 25 µl, keeping the same ratio of 5x sample buffer. All samples were then centrifuged briefly to collect the sample at the bottom of the tube, denatured at 100°C for 5 minutes and then centrifuged again briefly to collect the sample at the bottom.

SDS-PAGE gels were placed in running buffer (25 mM Tris-HCl, 190 mM Glycine, 0.1% (w/v) SDS) and prepared samples were loaded with up to 25 µl of the samples. Alongside Dalton Mark V11-L marker (66, 45, 36, 29, 24, 20.1, 14,2 kDa, Sigma) were run to allow an estimation of the protein sizes.

2.5.3 Electrophoresis

During the first 5 minutes, while the proteins passed through the stacking gel, the electrophoresis was run at a 100V. After this, the voltage was increased to 200V until the dye front reached the bottom of the resolving gel. The resolving gels were then carefully placed into a container to be incubated in either Coomassie Brilliant Blue R-250, SYPRO™ Ruby staining or silver stain. Alternatively the proteins were subjected to Western blotting. Only if indicated, the dye front was run off the gel in order to resolve higher weight proteins to a bigger resolution.

2.6 In-gel Protein Staining

Gels were minimally handled and stored in dust-free environments at all times so as to prevent tearing and contamination with keratin.

2.6.1 Coomassie Brilliant Blue R-250

Gels were removed from the running cassettes and placed into a plastic container and stained in 3 different Coomassie blue solutions. Sequential staining with these stains improves the sensitivity by gradually removing background. The staining solution was heated for 30 seconds in a microwave and the gel incubated for at least 30 min in the respective staining solution. Volumes used (100-500 ml) were appropriate for the size of the gel. After three Coomassie staining steps (Table 5), the gels were destained using destain. The gels were left in destain until all background staining had disappeared. The gels were stored in purified water before drying.

Table 5: Composition of the 3 Coomassie Blue R-250 staining solutions used. It has to be noted that the Coomassie Blue stock is composed of 1.25 % (w/v) Coomassie Brilliant Blue R-250 in dH_2O.

Ingredient	Coomassie I	Coomassie II	Coomassie III	Destain
Coomassie blue stock	2%	0.25%	0.25%	-
Propan-2-ol	25%	10%	-	-
Glacial acetic acid	10%	10%	10%	10%
Glycerol	-	-	-	10%

2.6.2 Disruptive silver

All solutions were prepared immediately prior to use. It should be noted that all procedures for disruptive silver staining were performed in a glass dish, since polycarbonate would interfere with the staining.

Gels were removed from the running cassettes, placed into glass containers and incubated twice in fixing solutions (40% (v/v) ethanol, 10% (v/v) acetic acid) for 30 minutes. Gels were then transferred for 30 minutes in sensitizing solution (30% (v/v) ethanol, 0.13% (w/v) glutaraldehyde, 6.8% (w/v) sodium acetate-three-hydrate, 0.2% (w/v) sodium thiosulphate pentahydrate) followed by three washes in dH_2O of 5 minutes each. The gels were then transferred into silver nitrate solution (0.1% (w/v) silver nitrate, 0.008% (v/v) formaldehyde) for 40 minutes, followed by brief washing with dH_2O and addition of developing solution (2.5% (w/v) anhydrous sodium carbonate, 0.004% (w/v) formaldehyde). The gel was left in the developing solution until bands of proteins were suitably visible with agreeable background. The gels were then transferred to fixing solution (1.46% (w/v) EDTA) for at least 1 hour.

2.6.3 SYPRO Ruby Red

SYPRO Ruby Red (Genomics Solution Ltd.) has a wide quantitative range, ranging from the lower limits of sensitivity of silver staining to the higher limits of Coomassie Brilliant Blue R-250 [73]. All steps were performed in a glass dish since polycarbonate interferes with the staining. The SYPRO stain was pre-filtered to remove any precipitate from it.

Gels were fixed twice in fixing solution (40% (v/v) methanol, 10% (v/v) acetic acid) for 30 minutes, followed by over-night incubation with the pre-filtered SYPRO staining. Staining solution was removed and the gel washed briefly with dH_2O. Then, it was incubated twice in destain (10% (v/v) methanol, 6% (v/v) acetic acid) for 30 min-1 hour. Gels were then imaged on the Typhoon 9140 Variable Mode Imager (Amersham Pharmacia Biotech, Inc., Uppsala SE-751 84 Sweden).

2.7 Bradford protein assay

The Protein Assay from Bio-Rad Laboratories (Bio-Rad Laboratories Ltd.) was used to determine protein content of ER preparations. The manufacturers' instructions were followed.

2.8 Mitochondria enrichment

The protocol for a dER preparation was followed. After the 2000 g centrifugation (and after removal of the fat pad), the protocol changed slightly, in that a 15 minute centrifugation step of the supernatant at 10,000 g in a Beckman F0650 rotor at 4°C in a Beckman Avanti 30 centrifuge was added. 1 ml of the supernatant of the 10,000 g centrifugation step were removed, and stored in aliquots at -80°C until needed.

2.9 Western blot

2.9.1 Electrophoretic Transfer

Proteins were run on a 1-D PAGE as described above and then transferred to a nitrocellulose membrane (Amersham Biosciences) using a Mini Protean II Western Transfer cell (Bio-Rad Laboratories Ltd.). The transfer was performed over 1h at 70V in transfer buffer (25 mM Tris-HCl pH 8.3, 0.15 M glycine, 10% methanol). The membrane was then transferred into a small quantity (about 10 ml) of Ponceau-S stain (0.1% (w/v) Ponceau S). The lanes and the marker are marked using a pencil.

2.9.2 Immunoblotting

The following steps were all done in a plastic dish under constant and gentle shaking. The membranes were blocked with blocking solution (2% (w/v) milk powder in Tris-buffered saline with Tween 20 (TBS-T: 20 mM Tris-HCl, 500 mM NaCl, pH 7.5, 0.1% (v/v) Tween 20) to prevent non-specific binding of antibodies. This was left to incubate for either 1 hour or overnight at room temperature. Afterwards the blocking solution was discarded and the membrane washed briefly with TBS-T and incubated for 1 hour in TBS-T containing the primary antibody at the relevant dilution. This was then discarded and the membranes washed thrice, to remove excess primary antibodies, in TBS-T for 15 min, 5 min and 5 min. Then the membrane was incubated in TBS-T containing the secondary antibodies of choice at the relevant dilution, (either anti-IGg anti-rabbit Cy-3 conjugated antibodies (dilution 1:5,000) or anti-IGg anti-rabbit horseradish peroxydase conjugated antibodies (dilution 1:20,000)), for 1 hour in the dark. The solution was then discarded and the membrane washed thrice with TBS-T for 15 min, 5 min and 5 min to remove excess secondary antibodies under normal light conditions.

2.9.3 Western blotting imaging with Cy-3 conjugated secondary antibodies

The membranes were washed three more times in TBS-T for 5 min each. In order to reduce background when imaging on the Typhoon Variable Mode Imager (Manufacturer: GE Healthcare Solutions), the membranes were kept under normal light conditions. Afterwards, the membranes were carefully placed on some tissue under the fumehood until the membrane was dry. Using the Typhoon Variable Mode Imager set to image in fluorescence using the Cy-3 filter, the images are taken at a resolution of 100 µm.

2.9.4 Quantitative analysis of Western blot that were incubated with Cy-3 secondary antibodies

The images of the Western blots with Cy-3 conjugated secondary antibodies were visualised in ImageQuant (manufacturer: GE Healthcare Solutions). The quantitation area was kept as small as possible and importantly similar in all measurements to be compared to each other. Using the volume report in Imagequant, the fluorescence of each band was evaluated. All measurements were done at leasts in triplicates with having a control run alongside for comparison.

2.10 Scanning Electron Microscopy

2.10.1 Preparing the SEM chips

9 silicon wafer chips (5 x 5mm) from Agar scientific (Unit 7, M11 Business Link Parsonage Lane, Stansted, Essex CM24 8GF England) were numbered using a diamond cutter according to Table 6. They were then cleaned in glass dish filled with acetone. The chips were then left to air dry underneath a fume hood. 10 µl of a 1mg/ ml polylysine solution were then dropped on each of the 6 chips. Using the pipette as spreader, the liquid was equally spread on the whole of the chip. The chips were then placed in a plastic Petri dish, covered and sealed, and incubated for 24 hours at 4°C.

2.10.2 Preparing the sample for SEM

Two pellets (out of six) from a fresh ER preparation (taken before the resuspension in glycerol) were needed for this experiment. One pellet was re-dissolved in 120 µl of 10% glycerol (w/v) using a yellow pipette to gently pipette the solution up-and-down to prevent frothing of the preparation. 10 µl were then taken out and diluted 10 fold with 10% glycerol in a clean eppendorf. A further 100 x dilution was then prepared from the 10x dilution, again using glycerol.

The other pellet was re-dissolved in 120 µl of pre-fix (80 mM PIPES (pH6.8), 1 mM $MgCl_2$, 150 mM sucrose, 2% (w/v) paraformaldehyde, 0.5% (v/v) gluteraldehyde) using a pipette to gently pipette the solution up and down to prevent frothing. A 10x and a 100x dilution were then made using pre-fix as diluent.

2.10.3 Loading the sample on the chips

The samples were loaded on the chips according to Table 6. 10 µl of the respective solution were placed on the respective silicon chips. All the chips were then left to incubate for 24 hours at 4°C.

Table 6: Table detailing the sample loading as well as the chip coating of all the chips prepared for SEM analysis.

Chip Nr	Amount to load	Loading	State of chip
1	10 µl	ER in 120 µl 10% glycerol	Not coated
2	10 µl	10 x dilution	Not coated
3	10 µl	100 x dilution	Not coated
4	10 µl	ER in 120 µl 10% glycerol	Polylysine coated
5	10 µl	10 x dilution	Polylysine coated
6	10 µl	100 x dilution	Polylysine coated
7	10 µl	ER in 120 µl pre-fix	Polylysine coated
8	10 µl	10 x dilution	Polylysine coated
9	10 µl	100 x dilution	Polylysine coated

2.10.4 Processing sample on silicon chips for SEM

The chips were placed in a glass Petri dish containing Karnovski's fixative (2% paraformaldehyde, 2.5% glutaraldehyde in 0.1M phosphate buffer (pH 7.4)) for 10 minutes. Remove chips to a Petri dish containing phosphate buffer (0.1M phosphate) and wash by gentle agitation for 5 min. The chips are then dehydrated by washing consecutively in water, 50%, 70%, 95%, 2x 100% alcohol for 2 min each. The Critical Point Dryer (CDP) carrier Bal-tec model 030 (Leica systems, Davy Avenue Knowlhill, Milton Keynes, MK5 8LB Bucks United Kingdom) was then placed in a dish containing 100% alcohol. Care was taken to immerse the whole carrier in alcohol. The chips were quickly transferred to the carrier to prevent drying out and the lid was placed on lining up the notches. The chamber of the Bal-tec CDP model 030 (Leica systems, Davy Avenue Knowlhill, Milton Keynes, MK5 8LB Bucks United Kingdom) was filled with 100% alcohol to the level of the exhaust pipe and the carrier was transferred.

2.10.5 Critical point drying

The lid of the Bal-tec CDP model 030 chamber (Leica systems, Davy Avenue Knowlhill, Milton Keynes, MK5 8LB Bucks United Kingdom) was tightly screwed on the chamber. After switching on, the cooling button was pressed. During the cooling period the valves of the attached CO_2 cylinder were turned on and "Medium in" was pressed. Once the chamber had reached a temperature of 10°C, "Medium out" was pressed and pressed again when the liquid fell to the top of the specimen carrier (leaving "Medium in" switched on the whole time to speed up the exchange). This step was repeated 15 times until no ethanol came out of the liquid exhaust tube. Leaving "Medium in" on, this was left to stand for 60 min and then the exchange procedure was repeated a further three times to make sure that no alcohol was present in the chamber anymore. The last time, "Medium in" was switched off when the liquid reached just below the top of the front window. After making sure all valves were closed, the CO_2 cylinder valve was closed. After waiting for the temperature to reach 40°C and checking that the gas valve was closed, "Gas out" was pressed. The gas Valve was gently opened until the gas flow meter showed 10. By gently adjusting the gas valve, the gas flow meter was kept around 10 until all of the gas had been expelled.

2.10.6 Chromium coating

The coating was done with a Cressington 308R Coating System, to which were attached a Cressington 308R 1000W Sputter Supply and a Cressington MTM thickness monitor (Cressington Scientific Instruments Ltd., 34 Chalk Hill, Watford WD19 4BX, England). The chips were then coated according to the manufacturer's instructions to 2 nm before being imaged under the microscope.

2.10.7 SEM imaging

The chips were then imaged in a Hitachi S-5200 Field Emission Scanning Electron Microscope Ultra-High definition (Hitachi High Technologies America, Ltd., 10 North Martingale Road, Suite 500 Schaumburg, Illinois 60173-2295).

Each of the three chips was then scanned for about 15 minutes under the microscope and pictures s, representing either vesicles or whole ER, were taken.

3. Results

3.1 Bioinformatics analysis of MudPIT data obtained from *Ricinus communis* developing seeds.

In 1997, Broun e al. [30] identified a cDNA encoding for the protein oleoyl-12-hydroxylase (EC number 1.14.13.-), responsible for the 12-hydroxylation of 18:1-cis-9 fatty acid in castor:

$$\text{oleoyl-CoA + NADH + oxygen + } H^+ \text{ <=> ricinoleyl-CoA + } NAD^+ + H_2O.$$

When inserting the hydroxylase cDNA into Arabidopsis using Agrobacterium, hydroxylase could be detected, showing that the cDNA was successfully translated. Also, it could be detected that 0.01% of ricinoleate were present in the seed oil [30]. As the ricinoleate content was so much lower than that observed in castor beans, the conclusion that can be drawn is that further proteins interact to produce the high yield of ricinoleate seen in the *Ricinus communis* seeds [37, 47, 74].

DGAT has been thought to be the rate limiting enzyme in TAG production [75]. Indeed downregulation of DGAT resulted in reduced TAG content, delayed seed development and altered seed FA composition [76] whereas overexpression enhanced seed weight and oil deposition [48]. It is thought that the DGAT of any particular crop will have structural features that will enable them to efficiently acylate with the predominant fatty acid. Castor bean DGAT predominantly inserts ricinoleate into DAG; however this preference for substrate was not exhibited by other DGAT (as they do not have ricinoleate and ricinoleate is not used as a substrate by non-castor bean DGAT), hence showing that Castor bean DGAT is selective towards ricinoleate [77]. The biosynthetic pathway in *Ricinus communis* has also been elucidated and steps that appear critical were elucidated [78]. Using only an

overexpression of oleate-12-hydroxylase using modern technics, a maximum of 17% of ricinoleate in seed oil content could be achieved [30, 79-81], far removed from the 90% that is achievable in castor bean. Burgal et al. postulated the hypothesis that the use of ricinoleate in TAG not only needed the evolution of hydroxylase from FAD2 but also another enzyme. When inserting RcDGAT2 into Arabidopsis as well as oleate-12-hydroxylase it was possible to show an increase from a maximum of 17% (seen in the other experiments) to nearly 30% [55]. Burgal also proposes the theory that the low ricinoleate oil seed content that was achieved up to date were caused partly to the lack of compatible TAG biosynthetic machinery and that further increase in oil seed content could be achieved by identification of enzyme activities that can incorporate ricinoleate into the glycerol backbone upstream of DGAT2 [55].

A comparison between a set of proteins identified using MudPIT in a storage-lipid producing *Ricinus communis* ER preparation (unpublished data) and a set of predicted ER proteins in a non-storage-lipid-producing Arabidopsis callus cell culture [65, 67] could lead to the identification of one of the target protein that are vital in increasing the ricinoleate yield in Arabidopsis.

Furthermore, a comparison between the proteome of an ER preparation and a set of proteins whose localization has been predicted in Arabidopsis will provide a qualitative analysis of the contaminant proteins of the ER isolation according to Simon et al. [2] used for the MudPIT analysis. This analysis, together with the analysis performed in the subsequent chapter will determine the amount of contamination to the ER preparation by Simon et al. [2].

3.1.1 Specific aims

- Identification of potential target proteins which are involved in ricinoleate biosynthesis by performing a bioinformatics analysis of existing data. The purpose of this would be to eventually incorporate these proteins into Arabidopsis, and eventually Brassica napus, to test whether they increase the ricinoleate content of seeds
- Analysis of the extent of contamination of the ER fraction, prepared according to the protocol of Simon et al. [2], with proteins from other sub-cellular locations.

Bioinformatic analysis relies on data from experiments. In this case, two datasets, from Dunkley et al. [65, 67] on Arabidopsis thaliana and from Simon (unpublished data) on *Ricinus communis*, previously generated in two different experiments will be compared. In order to understand the significance of the data obtained by each experiment and to follow logically the conclusions that can be drawn from this experiment, the two experiments that provided the data will be discussed below.

3.1.2 LOPIT

The Arabidopsis tissue culture LOPIT experiment has already been described in detail in chapter 1.5.1. Unfortunately, no LOPIT analysis of Ricinus has been done yet, therefore the need to compare an Arabidopsis proteome with a Ricinus ER preparation as presented in summary below and in chapter 1.5.3.

3.1.3 MudPIT experiment of ER from developing castor bean seeds

The experiment by Simon et al. described in chapter 1.5.3 will be used as comparator. The method described below was developed to allow the identification of target proteins that may be involved in ricinoleate production. A further search in the Uniprot database will elucidate previous work on these target proteins, thus validating further research into these proteins.

3.1.4 Results and discussions

The data obtained in [65] was classified according to the ER score of the proteins. Although the paper specified that all proteins with ER scores of 0.88 or higher could be considered as predicted ER, proteins down to an ER score of 0.5 were included. As the main aim was to identify potential protein candidates involved in the production of ricinoleate, this measure was taken to certify that even those proteins whose localization was unknown would be represented in the search for a protein candidate.

The data obtained in [67] was separated according to the predicted localization as determined by Dunkley et all. The list of ER predicted proteins was then pooled with the ER predicted localized proteins from [65] .

The sequence of each protein was then retrieved from the TAIR database (Table 4, item Nr 1) in a FASTA format. This sequence was then taken and, using the BLAST engine from the Ricinus webpage (WU-BLAST 2.0 with program set to blastp and database to "castor bean genes-proteins") (Table 4, item Nr 2), run against the Ricinus database (Table 4, item Nr 3). The top five results were then checked against the results of the castor bean ER MudPIT data. If one of the proteins was present in the castor data, then the rest of the five proteins were not checked. If a protein had been identified in the *Ricinus communis* ER MudPIT data, then the accession number of the protein, its BLAST score and the length of the original Arabidopsis protein were noted. If none of the first five Ricinus homologs (of the Arabidopsis protein) has been identified in the *Ricinus communis* ER MudPit data then the accession number of the highest scoring protein, its BLAST score and the length of the original Arabidopsis protein were noted.

The *Ricinus communis* ER MudPIT data was then analysed. The sequence of each protein identified was then retrieved locally from the Ricinus protein database (Table 4, item Nr 4) and then, using a BLAST program that was downloaded from the NCBI database (set to standard parameters in BLASTp mode) against the downloaded TAIR database (Table 4, item Nr 6). The top five Arabidopsis homologs (of Ricinus proteins) of each BLAST result were then searched against the results of the two Arabidopsis tissue culture LOPIT experiments [65, 67], unless the BLAST score of the proteins was below half of the top scoring protein. The same procedure was used to compile a list of Arabidopsis homologs

to the identified Ricinus proteins, with the exception that the Arabidopsis protein name was also added.

Research of function of proteins

A Bioinformatics search for the function of proteins that were present in the Ricinus data but not present in the Arabidopsis tissue culture LOPIT data was then done using the Uniprot database (Table 4, item Nr 7). The functions as well as their localisation were extracted from the gene ontologies. The functions were classified into several groups, out of which only those involved in lipid metabolism were further considered.

Table 4: Table of bioinformatics resources used. The" Nr item" refers to the number given to each resource in the above text. The "Data to download" refers to the exact data that was download from that webpage if several different items can be downloaded.

Nr item	Item	Website where to download it	Data to download
1	TAIR sequences	www.arabidopsis.org	
2	BLAST engine from Ricinus database	http://blast.jcvi.org/er-blast/index.cgi?project=rca1	
3	Ricinus database	http://castorbean.jcvi.org/	
4	Local Ricinus database	http://castorbean.jcvi.org/castorbean_downloads.shtml	Protein sequence (AA translation)
5	BLAST engine	ftp://ftp.ncbi.nlm.nih.gov/blast/executables/blast+/LATEST/	ncbi-blast-2.2.22+-win64.exe
6	Local TAIR database	ftp://ftp.arabidopsis.org/home/tair/Sequences/blast_datasets/TAIR9_blastsets/	TAIR9_cds_20090619
7	Uniprot database	http://www.uniprot.org/	

Combining the Arabidopsis tissue culture LOPIT data from 2004 and 2006, 228 Arabidopsis ER proteins were identified. As the Mudpit data looks at proteins from Castor bean, it is necessary to identify the Ricinus homologs of the Arabidopsis proteins. After identifying the Ricinus homologs (using BLAST) on the castor bean database of these 228 proteins, the homologs were compared to the data obtained in the MudPIT ER experiment. Out of the 228 proteins, 95 Ricinus homologs were not detected in the MudPIT data, while 133 homologs overlapped with the MudPIT data. This means that out of the 404 ER proteins that were discovered in the MudPIT experiment, 271 novel ER proteins could be discovered. Hence the technique used in the MudPIT ER experiment can be described as able to identify more ER proteins than the LOPIT technique, taking into account the downfalls of doing the experiment using different plants as starting materials as well as the possible contamination of the ER used in the MudPIT experiment. The results have also been presented in a diagrammatic form in Figure 6.

A total of 336 proteins were identified in the first MudPIT experiment (without SDS) and 159 were identified in the second MudPIT experiment (with 0.2% SDS). Out of those 159 proteins, 68 proteins were identified that were not identified in the first MudPIT experiment. Therefore a total of 404 novel proteins were identified in the ER. Out of the 402 Arabidopsis homologs found (two proteins did not have any homologs), 220 were not present in the Arabidopsis tissue culture LOPIT data (data not shown) and 184 were present. The function and localisation data for these proteins was then searched on Uniprot and classified into groups according to their function. Only 5 proteins could be shown to be involved in storage lipid synthesis, fatty acid biosynthesis and triacylglycerol assimilation (Table 1). As the nature of the protein that is being looked for is completely unknown, any protein that is identified in the lipid pathway and present in the ER needs closer study. Due to their known localization and their known function, these may be potential protein targets. Literature present on the function of these proteins was analysed and will be presented below. The

results of the bioinformatics analysis have also been presented in a diagrammatic form in Figure 7.

In 2006, Rahier et al [84], while studying the sterol biosynthesis pathway in Arabidopsis, isolated two cDNA encoding for bifunctional 3-hydroxysteroid dehydrogenase/C- 4decarboxylases (3βHSD/D), termed At3βHSD/D1 and At3βHSD/D2. It could be determined that these proteins are ER-resident (they contained an ER-targeting C-terminus), they were proven to be of vital importance for the sterol production in Arabidopsis. Erg 26 mutants, lacking 3βHSD/D activity, could be restored to normal growth and ergosterol synthesis by the transformation of with At3βHSD/D cDNA. Sterol being important in membrane lipid composition, this enzyme was probably wrongly classified in the Uniprot database. This enzyme can be excluded as being a target protein, as it is involved in a completely different pathway than storage lipid synthesis.

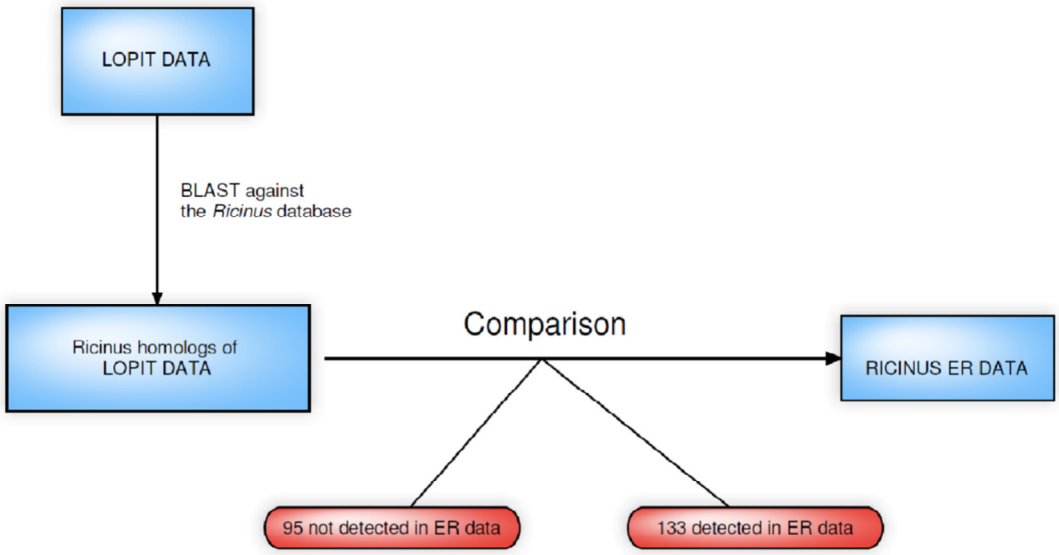

Figure 6: Flow diagram summing up the results of the comparison of the Ricinus homologs of the Arabidopsis tissue culture LOPIT data against the Ricinus MudPIT ER data.

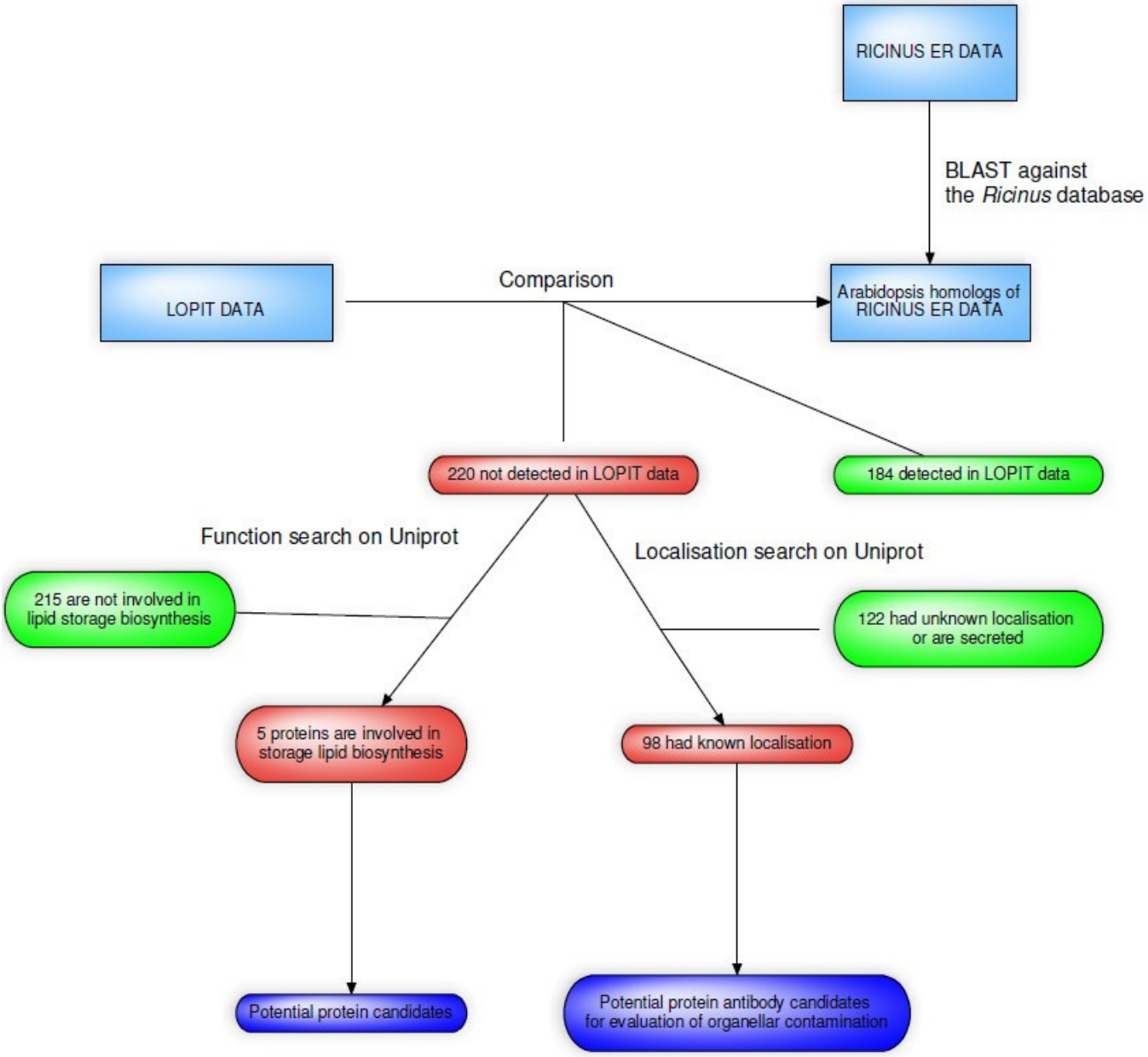

Figure 7: Flow diagram summing up the results of the comparison of the Arabidopsis homologs of the Ricinus MudPIT ER data against the Arabidopsis tissue culture LOPIT data.

3-oxoacyl-(acyl-carrier protein) reductase could not be identified in the Arabidopsis tissue culture LOPIT experiment, however it was identified in the MudPIT of the ER preparation. Uniprot listed its localisation as chloroplast envelope. Since metabolic channelling is thought to be involved, any protein that is present in the membrane of another compartment than ER may also be interesting since it could interact with the membrane-localised hydroxylase. However, another name for 3-oxoacyl-(acyl-carrier protein) reductase is βKR [85] which has been encountered beforehand in chapter 1.3.1. It is part of the fatty acid biosynthesis machinery of the plastid (chloroplasts are variation of plastids). It is also soluble hence may be a contamination of the ER preparation. For these reasons this protein cannot be considered as a target protein which may be involved in producing the high ricinoleate content in castor bean seeds.

FAD2 is a well-known enzyme involved in storage lipid biosynthesis. Its function has already been reviewed in chapter 1.3.2. It cannot be considered as a protein target since it is already known and utilized in Arabidopsis [37]. Furthermore, it was discovered that FAD2 presents strong homology to hydroxylase [29]. Its detection in the *Ricinus communis* ER preparation is therefore normal. It too cannot be regarded as a target protein, mainly because it is already known to be involved in ricinoleate biosynthetic pathway.

A lipase is used during the breakdown of TAG to produce usable energy. They have already been isolated from different species like maize [86] or *Ricinus communis* [87]. It is quite clear that this category of enzymes is involved in the breakdown of TAG and not the biosynthesis of it. Its presence in the *Ricinus communis* ER MudPIT data is easily explained in that both ER extracted from developing as well as germinating castor beans were analysed by MudPIT. Since lipases are only transcribed when the TAG is broken down during germination or end of seed development, and a germinating ER prep was also analysed, its presence in the data is normal. It was probably insufficiently described in

Uniprot therefore was flagged up as a potential protein candidate. However, after further analysis of its function [88], it can be discarded.

The last protein that was flagged belongs to the DGAT family. Its exact role has already been described in detail in chapter 1.3.4.1, and will not be described here again. It can also be discarded as novel protein candidate because it has been known to be involved in TAG production [47].

It can be concluded that the bioinformatics approach of comparing the proteome of a storage lipid producing organelle with the predicted proteome of the same organelle (but storage lipid non-producing) did not reveal any new protein candidates which could increase the ricinoleate yield in Arabidopsis seeds. On the other hand, 40 proteins where identified whose localization was either ER or unknown and whose function was unknown. It could be possible that one of these proteins is a novel candidate protein. An extensive search for information in different databases on these proteins revealed that these have not been studied yet ie there is no information available. Extensively studying these proteins goes far beyond the scope of this thesis. The only way to reduce the number of potential protein candidates would be to investigate into the proteins with ER localization and unknown function. This could be done, for example, by isolating the proteins using one of the forms of liquid chromatography and then testing the enzymatic properties of these enzymes or by cloning these into a different system and looking at changes in the system. Another approach for identifying possible function would be to do active site homology searches in order to elucidate functions.

The proteins that could not be identified in the Arabidopsis tissue culture LOPIT paper were then classified according to their predicted localization. An overview of the proteins whose localization could be identified is presented in Table 7.

As argued beforehand, LOPIT is just a localisation prediction method. Therefore, as it is shown in the 2006 paper [67], LOPIT is not proof of localization but merely a prediction.

Also, it has to be taken into account that no purification can be 100% pure. Therefore any proteins that were not identified in the LOPIT paper however in the MudPIT data may not be localized in the ER. It could be that these are just normal contaminants (which may be variable depending on the preparation method used) as proteins released from other broken organelles may bind to the outside of the endoplasmic reticulum or it may be that other organelles co-purified along with the ER.

Table 7: Table showing the results of the bioinformatics analysis with respect to identifying potential protein candidates. The proteins that were identified in *Ricinus communis* are shown on the left. Care has to be taken considering the Ricinus name of the protein, since these have been proven to be wrong sometimes. The next column then looks at the result of the BLAST comparison to an Arabidopsis database and lists the accession number and the name of Arabidopsis equivalent. The "Function" column then describes broadly the function that this enzyme has. The "Localisation in Arabidopsis" column describes the localization of the protein as presented in the Gene Ontology section of the Uniprot database.

Accession	**Name**	**Arabidopsis equivalent**	**Name of Ara equivalent**	**Function**	Localisation in Arabidopsis
29739.m003645	NAD dependent epimerase/dehydratase, putative	AT2G26260.1	3beta-hydroxysteroid-dehydrogenase/decarboxylase isoform 2	Lipid synthesis	ER
27572.m000157	acyl-CoA dehydrogenase, putative	AT1G24360.1	3-oxoacyl-(acyl-carrier protein) reductase	Fatty acid biosynthesis	Chloroplast envelope
28035.m000362	oleate 12-hydroxylase	AT3G12120.2	fad2 (fatty acid desaturase 2)	Fatty acid biosynthesis	ER
30183.m001305	triacylglycerol lipase, putative	AT3G14360.1	lipase class 3 family protein	TAG production	Not known
29682.m000581	diacylglycerol O-acyltransferase, putative	AT3G51520.1	diacylglycerol acyltransferase family	TAG production	Not known

The information obtained through public databases has to be treated with some care since Uniprot presents the data from both Swiss-prot and TrEMBL. Although Swiss-prot is manually reviewed, TrEMBL is automatically reviewed, possibly introducing more errors into the data. Furthermore, the localization data was obtained for Arabidopsis and therefore may not apply to Ricinus.

In order to detect proteins by mass spectrometry a peptide has to be ionized, which is one of the main downfalls of the technique, as not all proteins produce peptides that can ionize. Hydrophobic peptides are especially difficult to detect on the mass spectrometer because of this problem. Although this is a downfall of the technique, it cannot be controlled for and has to be taken into account when evaluating the data concerning contamination. This may mean that neither all the ER proteins could be identified (especially concerning membrane proteins) nor all contamination could be determined.

As can be seen in Appendix A, the localization of these proteins is heterogenous. Two explanations can be found for this: 1) only a few proteins from different organelles co-localised with the cytoplasmic side of ER membrane proteins when the membranes of organelles (other than ER) were broken, 2) other organelles co-purified alongside ER but most of their proteins could not be detected by mass spectrometric means, either because the organelles where present in low concentration or because the peptides were not ionized. The qualitative information gained by performing a MudPIT experiment as well as a bioinformatics analysis of the comparison presented in chapter 3.1 will be used to select organelle markers. Using quantitative Western Blotting, it will be possible to evaluate if whole organelles co- purified along with ER.

3.2 Purity determination of developing castor bean ER preparation

3.2.1 Introduction

Inside the cell, proteins are usually separated into organelles (and cytosol) by membranes. Therefore the proteins within different organelles are spatially separated from each other and cannot interact. However, the preparation of a tissue for organelle isolation results in the breaking of cell membranes by mechanical force, which may also break organelle membranes. Proteins, that have an innate affinity for each other but that have been kept in a spatially separate location and therefore were unable to interact, can now interact. Intermolecular forces then allow proteins from different compartments to stick together. Therefore no pure organelle can ever be obtained using present techniques [89-91].

The LOPIT technique described in the previous chapters looks at this problem [65, 67]. By analyzing the distribution patterns of proteins of unknown localization on a continuous pattern and comparing it to the distribution patterns of proteins of known localization, Dunkley et al. were able to predict the localization of unknown proteins. This analysis showed that proteins do not separate along a continuous gradient according to the density of their organelles [65, 67].

Analysis of the MudPIT experiment done in triplicate on a purified ER fraction revealed 79 proteins whose known localization is not ER and 14 proteins whose known localization is ER. It indicates that at the conditions present, proteins from other organelles could be identified.

However, mass spectrometry is not quantitative, therefore it is unknown in what concentrations these proteins were present.

The possibility remains that the proteins identified belong to the most abundant proteins of the organelle it is localised in, and that, instead of only a single protein contaminating the ER preparation, the whole organelle co-purified as well, however only the most abundant one was identified. Definite evidence could be obtained by running the ER preparation on a further continuous gradient and seeing whether any further bands are produced as well. However, when tried in triplicate, by Adrian Brown and the author (unpublished data) using a continuous iodixanol gradient, the ER did not enter the iodixanol gradient when centrifuged for 18 hours at 150.000 g. Hence the technique presented below has to be applied to determine if contaminating organelles purified as well.

Western blotting is a technique that utilizes the binding of antibodies to specific antigens to identify a protein in a complex mixture. Several techniques of antibody detection exist, however the only one relevant to this work is the use of Cy-3 conjugated secondary antibodies. A useful property of Cy-3 is that it is fluorescent. By washing off the non-bound antibodies and then analysing the membrane for fluorescence, it is possible to identify bound primary antibodies (since secondary antibodies are bound to it). An advantage that the Cy-3 technique has over the other techniques is that it allows the relative quantification (the comparison) of several samples. The fluorescence volume increases proportionally with the amount of secondary antibody bound, which is related to the amount of antigen [92].

A classical method to prove purity of an organellar purification is to do Western blots using antibodies against organelle marker proteins [90]. If the marker protein is present in the purified or enriched sample, then it could be possible that the whole organelle, of which the protein is a marker, has also been separated.

.

3.2.2 Specific aims

- To determine the degree of contamination present in an ER enrichment experiment prepared according to Simon et al. [2].
- To determine the nature of the contamination of a developing castor bean ER prep, as according to Simon et al. [2], from an organellar perspective.
- To determine quantitatively the contamination of a developing castor bean ER prep with the purpose of identifying the confidence in results that could be achieved if performing an ER membrane topology experiment
- To determine the confidence in the results of the MudPIT experiment done by Simon et al. (unpublished data).

3.2.3 Results

The method used for ER enrichment, developed by Simon et al.[2], relies on discontinuous density gradient centrifugation. Unlike a continuous gradient, where the position of an organelle is representative for its density, organelles are collected in a discontinuous gradient at the interface between two different concentrations of a solution, which represents filters for different densities. Although it facilitates the identification and the extraction of the organelles of choice (they locate at the interface between two sucrose solutions of different density), the technical problems of creating two sucrose layers makes it a necessity for the two sucrose solutions to have a relatively large difference in density. This means that the specificity of organelle separation is lower in discontinuous gradients than in continuous gradients. All organelles that have a density in between the two different density sucrose solutions would co-purify. It is therefore important to show that indeed only the right organelles were isolated and that these are not contaminated by whole unwanted organelles which co-purified alongside them.

Although the following analysis will in itself only give information on the contamination by a few select proteins, an analysis in conjunction with the data obtained from the bioinformatics data as well as comparison with literature on proteomic studies will allow a qualitative and quantitative analysis of contamination.

Knowing that hydroxylase is present only in ER[30], an antibody against hydroxylase can be used to monitor the ER preparation. Using anti-hydroxylase antibodies as ER marker in a Western Blot, a comparison between equal loadings (10µg) of the supernatant of a 300 g spin of a homogenate and a dER prep of the same batch showed a strong enrichment of ER in the developing ER preparation (Figure 8).

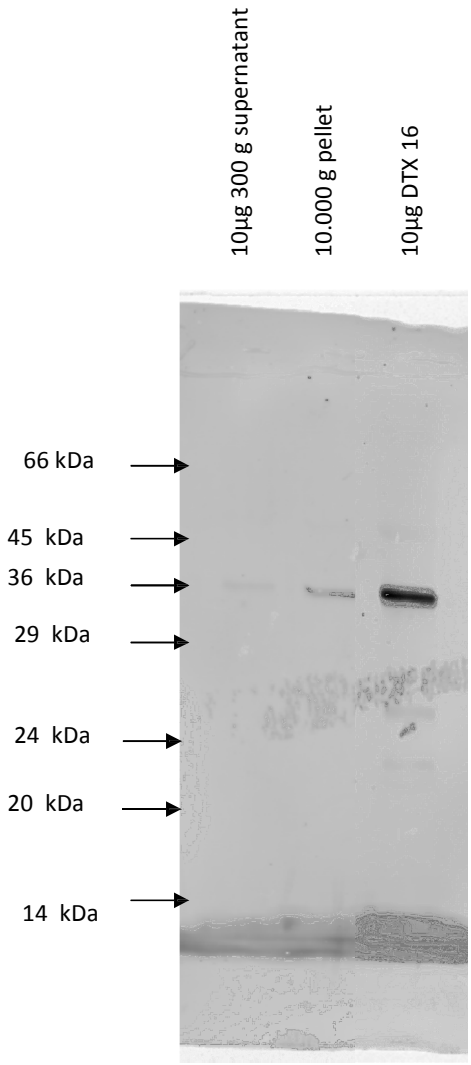

Figure 8: WB using anti-hydroxylase primary antibody and a Cy-3 anti-rabbit conjugated secondary antibody used on samples taken from the same preparation. Each lane was loaded with 10µg protein, as determined by using a Bradford Protein Assay (Bio-rad Laboratories Ltd). The cross-reacting bands are at a size of 36 kDa, which corresponds to the size of hydroxylase. The band in the DTX 16 lane shows a much stronger signal than the 300 g supernatant, indicating enrichment has occurred. The 10.000 g pellet sample was included to show the necessity of the sucrose gradients in the prep.

Further analysis of the blot on the amount of fluorescence present in each lane showed that 58 times more hydroxylase was present in the developing ER prep than in the homogenate, indicating an enrichment of ER (Table 8) by 58 times. It is possible that not all the proteins transferred from the gel to the membrane, however this is unlikely since 1D protein gels of ER preps do not show a major band at 36 kDa when staining with SYPRO Ruby red(data not shown).

Table 8: Volume report of the hydroxylase western blot.

Name	Volume	Percent of detector saturation
300 g pellet	613004.6	1.59
10.000 g pellet	2241186	5.81
DTX 16	35741544	92.6

The amount of fluorescence present in each lane is analysed and represented in the column "Volume", while the column "Percent" represents the percentage of the measuring area that is filled with fluorescence. As long as this doesn't reach 100 %, the area measured was big enough and therefore the measurement is valid. Furthermore it has to be noted that the areas measured were the same for each lane. The amount of fluorescence is 58 x higher in DTX 16 than in the homogenate. This shows that indeed an enrichment has occurred.

Some of the proteins identified are protein markers [93]. The proteins discovered, Voltage-dependent anion channel (VDAC) and malate synthase (MAS), are markers

for the mitochondria and the peroxisome, repectively. The presence of the marker protein of the peroxisome in the ER prep can be considered as normal: the peroxisome originates from the ER and the proteins identified may just have been produced in the ER and belonged to peroxisome in the process of separating from ER [94-96].

Voltage-dependent anion channel (VDAC) proteins are porin-type β-barrel diffusion proteins. They are prominent in the outer mitochondrial membrane and facilitate metabolite exchange between the organelle and the cytosol. Using transient expression of fluorescent-tagged proteins, it was possible to determine that this membrane protein localises only to the mitochondrial outer membrane [93]. It therefore can serve as an organelle marker. Furthermore, VDAC was identified in the MudPIT experiment, therefore making it unlikely that a cross-reaction of the antibody is responsible for the signal detection at the right size of VDAC.

Using an anti-VDAC antibody as primary antibody and an anti-rabbit IgG Cy-3 conjugated secondary antibody, a Western blot was made of the homogenate of developing castor bean endosperm, an enrichment of mitochondria and of a range of dER preparations (Figure 9). The dER preps were made at different time points by different staff at the University of Durham using the same protocol from Simon et al. [2]. The protein content of all the samples were determined using a Bradford Protein Assay (Bio-rad Laboratories Ltd) and 10 µg of protein were loaded into each lane. dER 25 was produced in 02.10.04 by Dan Maltman and Steven Gadd. dER 63 was produced in 02 May 08 by Joanne Robson. DTX 16 was produced on the 05 Aug 09 by the author of this thesis.

The blot showed that a signal could be obtained in the 300 g supernatant, which was amplified in the 10.000 g pellet (enrichment in mitochondria), therefore indicating that indeed a mitochondrial protein has been identified (Figure 9).

A volume report on the Typhoon (Table 9) showed that more fluorescence (therefore more VDAC protein) is present in the enriched fraction (10.000 g pellet) than in the homogenate (300g supernatant). This indicates that indeed a marker for mitochondria has been targeted by the antibodies. However, when looking at the dER 63 fraction and at the DTX 16 fraction, these show a higher fluorescence (therefore more proteins is present) than the enriched fractions.

Furthermore, when comparing the fluorescence of dER 25, DTX 16 and dER 63 a big difference can be seen in the measurement. Although DTX 16 and dER 63 show a difference of 21% in the total amount of fluorescence, which can be, due to the small sample size, explained by experimental or biological variation, the 1100% variation between dER 25 and DTX 16 cannot be explained by experimental or biological variation. Hence, the starting material must have been different.

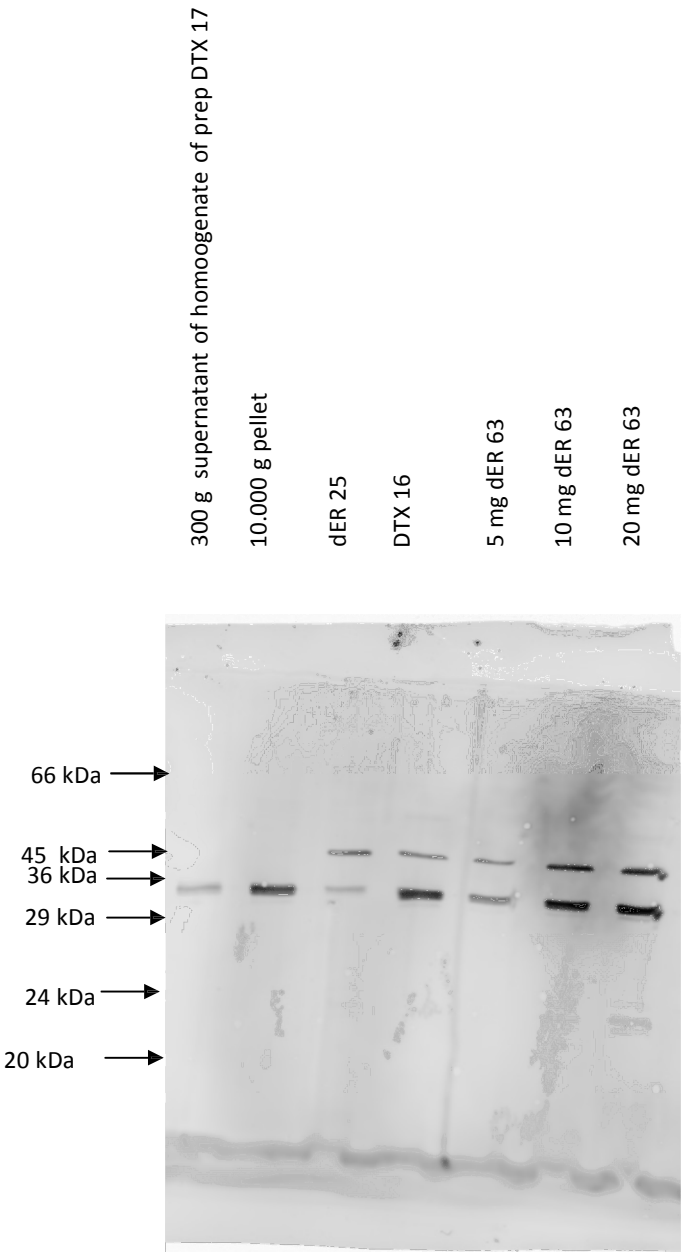

Figure 9: Picture of Western blot of a range of dER prep using anti-VDAC as primary antibodies. The image was taken at 470 V PMT on a Typhoon. A signal was detected at about 32 kDa. Although the protein was predicted, by the AA sequence, to be 29.5 kDa, it could have been post-translationally modified. The 10.000g pellet, which represents the enrichment in mitochondria, shows a far stronger signal than the 300 g supernatant. The band at 45 kDa is probably due to a cross-reacting protein, which has been concentrated during ER purification. dER 25 exhibits a stronger signal at 45 kDa than at 32 kDa. In the other preps it is exactly the opposite, therefore it can be concluded that dER 25 is different. This is easily explainable by the plants being kept under suboptimal growth conditions which has led to different protein expression within the cell.

Table 9: Volume report of fluorescence of the above blot. It can be noticed that the 10.000g pellet (which is enriched in mitochondria) has a 7x stronger signal than the 300g supernatant. It can be seen that dER 25 contains 1.36x less fluorescence than the 300 g supernatant, therefore less mitochondrial marker than the homogenate. DTX 16 contains an 8x stronger signal than the homogenate. 10µg dER 63 has a 11 x stronger signal than the 300 g supernatant. Both the 10 µg DTX 16 and the 10 µg dER 63 have a stronger signal than the 10.000g pellet, the enriched fraction.

Name	Total fluorescence	Percent of maximal fluorescence
20 µg dER 63	31972391	29.06
10 µg dER 63	28244580	25.67
5 µg dER 63	6464014	5.87
10 µg DTX 16	20764794	18.87
10 µg dER 25	1923309	1.75
10 µg 10000 g	18065989	16.42
10 µg 300 g sup	2592988	2.36

One of the uncontrollable variables is the growth and development of living material. Although these are controlled for as much as possible in keeping the growth temperature, light intensity, amount of water supplied as well as the growth of seeds from only one seed batch constant, a complete control of these factors is not achievable due to biological variation. As described in the method chapter, all the plants were kept at constant temperature and under controlled light/dark schedule. The protocol that is currently used (that has been used since 2005) can be considered as optimal.

The dER prep from Dan Maltman (dER 25) showed a very different blot to the two other dER preps. The upper band, at 45 kDa, shows a much stronger signal, than the VDAC band at about 32 kDa. This can be compared to the signal in the more recent prep dER 63 and DTX 16. In both of the other preps, the signal of the 45 kDa band is weaker than the signal of the VDAC band. No evidence suggests that the 45 kDa band has anything to do with VDAC, but rather that it is a cross-reaction of the anti-body with an ER protein, which only shows up in purified ER fractions (http://www.agrisera.com/en/artiklar/vdac1-voltage-dependent-anion-selective-channel-protein-1.html.

This indicates that the dER prep 25 is different from the other two preps. An explanation for this would be that the plants were not kept under optimal conditions (the optimal growth conditions were only elucidated sometime after dER 25 was produced). They were smaller in appearance and produced less seed than when they are kept under the optimal conditions instigated at a later date.

Therefore the results obtained with the dER 25 were excluded from the data analysis.

3.2.4 Discussion

Figure 8 shows that the protocol gave an enrichment of ER, resulting in 58x more hydroxylase proteins in the dER prep than in the homogenate. From this, as well as the high number of ER proteins that were identified in a MudPIT experiment from Simon et al. [2], it can be concluded that there was an enrichment of ER organelles during the isolation procedure.

The total fluorescence of the VDAC blot showed that DTX 16 and dER 63 show a higher amount of fluorescence than even in the mitochondria-enriched sample. One of the explanations for this could be that VDAC has an affinity for some protein in the ER of developing seeds.

Therefore, as soon as the mitochondrial membrane, which kept the proteins physically apart, is burst during homogenization, it binds to some protein on the ER. When now enriching in ER, the VDAC protein, attached to some protein from the ER, will also be enriched. In order to efficiently test for this co-localization of proteins, one would need to obtain quantitative results with a further plant mitochondrial marker, which has not been done due to the limited scope of this thesis.

Another explanation could be that the whole mitochondria are isolated at the same time as the ER. However, this is relatively unlikely. Although some mitochondrial proteins were identified by MudPIT, not enough were identified to suggest that whole mitochondria are present in the dER prep. In 2001, Millar et al. [97] did a proteomic analysis of the mitochondrial proteome and identified 100 high-expression and 250 low-expression proteins. This stands in contrast to the non-quantitative identification of 13 mitochondrial proteins in the MudPIT data from Simon et al. [2]. Furthermore, Kruft et al. [98] determined that the purity of mitochondrial enrichment fractions can be determined by the detection and relative quantification of mitochondrial specific complexes (the NADH dehydrogenase, the HSP60 complex, the F0F1-ATP synthase (partially dissociated into the F1 and F0 parts), and the cytochrome c reductase). Although these complexes were identified in the Kruft et al. paper using 2D-PAGE, if the mitochondria had co-purified with the ER fraction , these should have been detected in the MudPIT data, especially since the concentration of the mitochondrial marker VDAC in the ER prep is at least 5x higher than in the homogenate (as determined by comparison of the volume report between 5 µg dER 63 and 10 µg 300 g supernatant.), while the purification of mitochondria.

The third explanation is that the VDAC antibody cross-reacted with some unknown protein that isn't VDAC, resident in the ER. This explanation is rather unlikely because VDAC was identified

in the MudPIT data. Considering that the signal band that is seen in the dER lanes is at exactly the same molecular weight as it should have been, this is rather unlikely. In order to get absolute certainty that the antibodies reacted with the right protein, a comparison using a 2D-PAGE Western Blot between 300 g homogenate and dER 63 needs to be done, followed by MALDI-TOF-TOF analysis of the identified protein.

To sum up, it can be said that there was an enrichment of dER (Figure 8), as demonstrated using the anti-hydroxylase antibodies. However, an exact number of the increase in hydroxylase cannot be obtained yet. Due to time restraints, Western Blot which tests the linearity of the fluorescence as with respect to overloading the nitrocellulose membrane could not be performed yet to confirm the 58x enrichment of hydroxylase.

Using anti-VDAC antibodies, it was possible to determine that a positive signal could be obtained in the homogenate(Figure 9). This signal increased in the mitochondria enriched fraction, therefore indicating that the VDAC antibody does indeed recognize a protein located in the mitochondria. It may be that the anti-VDAC antibody did recognize some other proteins (as the preparation was a 300 g homogenate which is supposed to rudimentarily concentrate organelles of the same density (or higher) than mitochondria). Furthermore, it was possible to determine that the dER 25 sample looked distinctly different from DTX 16 and dER 63. Considering that the plant growth protocol was not perfected then, the results for this sample (dER 25) were discarded. Together with the data obtained from the bioinformatics analysis of the MudPIT experiment by Simon et al. [2], it was possible to prove that the contaminations seen in the MudPIT data were not due to the co- purification of unwanted mitochondria but rather contamination that cannot be avoided. It has to be taken into account that *Ricinus communis* is not a plant that is used commonly in the lab. Therefore relatively few antibodies against organelle markers exist for Ricinus communis. Cross-reactivity between Arabidopsis and Ricinus was taken into account in this thesis. 5 further organelle markers, which were

developed for Arabidopsis, were tested out on homogenate as well as enriched samples and none worked. However, when tested against Arabidopsis samples, all of these worked (data not shown). Due to economic reasons, further analysis of the ER prep with regard to organellar contamination was not carried out. Considering that most proteins that were recognized in the MudPIT experiment, and whose localization was known, did show the same localization distribution pattern as VDAC, the conjecture that no other organelle co-purified together with ER can be made. In essence, it can be said that ER was purified 58x and mitochondria was purified 5x when compared to homogenate.

It can be concluded that the pre-requirement of low organellar contamination for an ER membrane topology elucidation has been met. No organelle seems to have co-purified alongside ER and therefore a membrane topology experiment would only elucidate the topology of ER and not that of any contaminating organelle as well.

Since the technique used does not absolutely quantify contamination, it can be said that 10x more VDAC is present in the dER preps than in the homogenate.

An exact number cannot be placed on the amount of contamination from the other proteins (because MudPIT is not quantitative), however when doing an ER topology experiment, the knowledge that contamination can only be present on the cytosolic side of the membrane allows easy exclusion of the contaminating proteins in the presentation of topology data .

Unexpectedly, in the Western Blot using anti-VDAC as primary antibody, the 32 kDa band showed a stronger signal in dER 63 and DTX 16 than in the mitochondrial enrichment sample. These experiments would not be determinant as to the feasibility of an ER membrane topology elucidation and therefore are not within the scope of this thesis.

3.3 Scanning electron microscopy analysis of a dER prep

Membrane topology can be determined by using a protease protection strategy. This involves the digestion of the cytosolic side of the membrane protein with a protease. The sealed membrane prevents the protease from entering the organelle and digesting the lumenar proteins. By re-isolation of the organelle which had its outside proteins digested, followed by lysis of the membrane and subsequent digestion of proteins using a protease, it is possible to distinguish between the cytosolic side of membrane proteins and the lumenar side. For this strategy to lead to the elucidation of membrane topology, two vital requirements need to be met.

One of the requirements is that the organelle whose topology is to be studied to be present in a highly enriched state. As was determined in the previous chapter, this requirement is fulfilled.

The other requirement is that the organelle to be analysed is present in a whole state, i.e. its membranes are still intact, in order to perform a protease protection strategy. It lies in the nature of membranes to have the tendency to form sealed bilayers. Small tears in the membrane continuity will, due to the thermodynamics of lipid bilayers, immediately be closed, thereby keeping sidedness and intactness of membrane [32] (p621). Therefore, the organellar membrane is able to compensate small tears in the membrane, which may occur during preparation, and no lumenar proteins would be lost and the structural proteins (which give the organelle its structure, hence its appearance under an SEM) would still be intact. Therefore, the organelle should, if looking at it under an SEM, have a distinct and complex structure.

In order to fully appreciate the relevance of the experiment done, it is of importance to understand the technology behind SEM. It has to be noted that a full review is far beyond the scope of this thesis and is covered in [99, 100].

Using SEM, it is possible to observe heterogeneous organic and inorganic materials on a nm to µm scale. The area to be examined is irradiated with a tightly focused beam of electrons, which may be swept in a raster across a surface to establish a high-definition image. Hence it should be possible to determine the appearance of the ER using SEM should the ER still have a complex structure.

It can also be the case that the shear forces exerted on the organelle during preparation exceeded the self-repair ability of the membrane. This would lead to the formation of membrane sheets. Membrane sheets being thermodynamically unstable (because hydrophobic molecules at the end of membrane sheets are exposed to hydrophilic molecules), these would form into vesicles. ER in the form of vesicles would be distinguishable under an SEM since it will have lost their ER-typical structure (arrangement of tubules and sheets [101]). Vesicles would be identifiable by their round structure. By comparison with current literature [101] (unpublished data from Goldberg), the difference between whole ER and vesicles would become immediately apparent under an SEM.

Although the existence of vesicles would not hinder the performance of a protease protection strategy (since they still represent a closed membrane), any membrane topology would be lost. During the formation of vesicles, the membrane has only a 50/50 chance of closing the right way around. A 50/50 mixture of ER membranes showing either the lumenar or the cytoplasmic side to the protease will mean that the peptides that will result from digestion will be either from the lumenar or cytoplasmic side of the organelle.

An analysis of the surface structure of isolated ER will therefore reveal if the ER is still intact or if vesicles have formed, thereby making an ER membrane topology experiment not possible.

3.3.1 Specific aims

To identify the structure of the ER in an ER preparation produced according to the methodology developed by Simon et al. [2]

3.3.2 Results

Images were taken of a single dER preparation prepared according to Simon et al. [2] which was subjected to three different treatments (Table 10). The pictures taken during analysis will be presented below. It has to be taken into account that only the 1/10 dilution was analysed in the SEM.

Table 10: Treatments of the analysed dER samples, prepared according to Simon et al. [2].

Treatment nr	Chip nr	Uses of fixatives before drying	Chip coating
1	2	No	No
2	5	No	Poly-lysine
3	8	Yes	Poly-lysine

A)

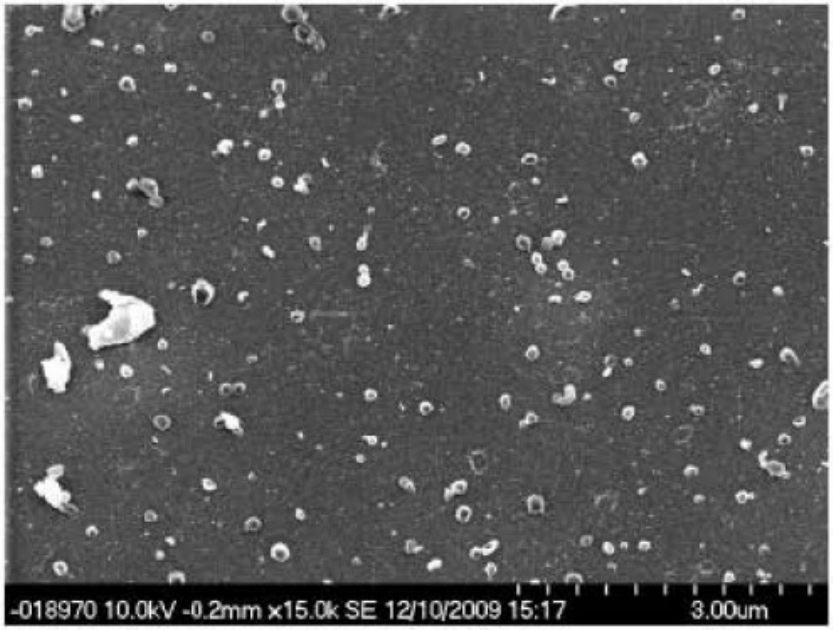
-018970 10.0kV -0.2mm x15.0k SE 12/10/2009 15:17
3.00um

B)

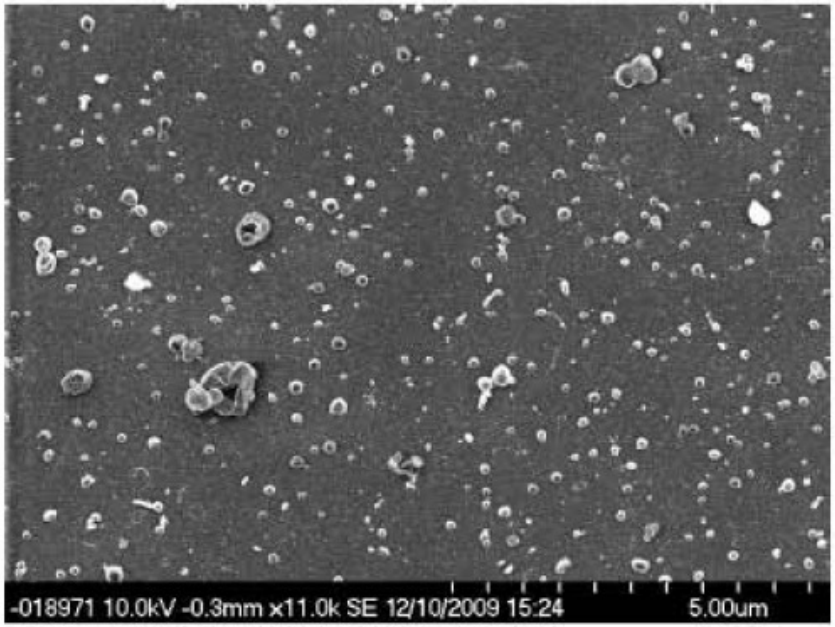
-018971 10.0kV -0.3mm x11.0k SE 12/10/2009 15:24
5.00um

C)

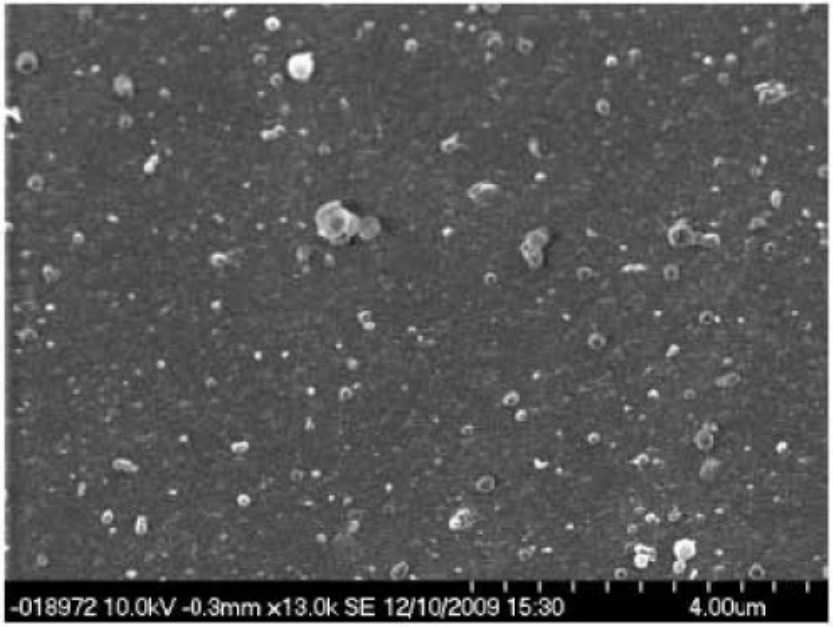
-018972 10.0kV -0.3mm x13.0k SE 12/10/2009 15:30
4.00um

D)

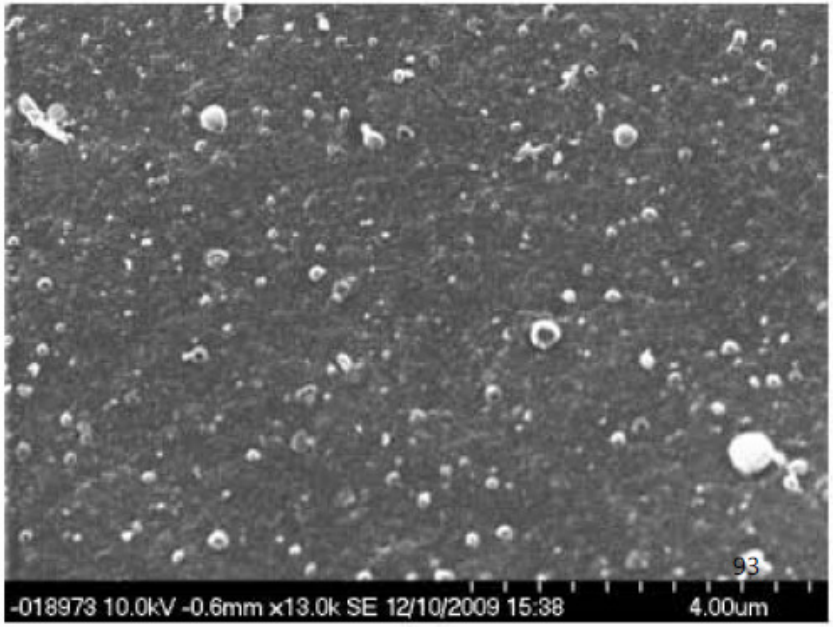
-018973 10.0kV -0.6mm x13.0k SE 12/10/2009 15:38
4.00um

E)

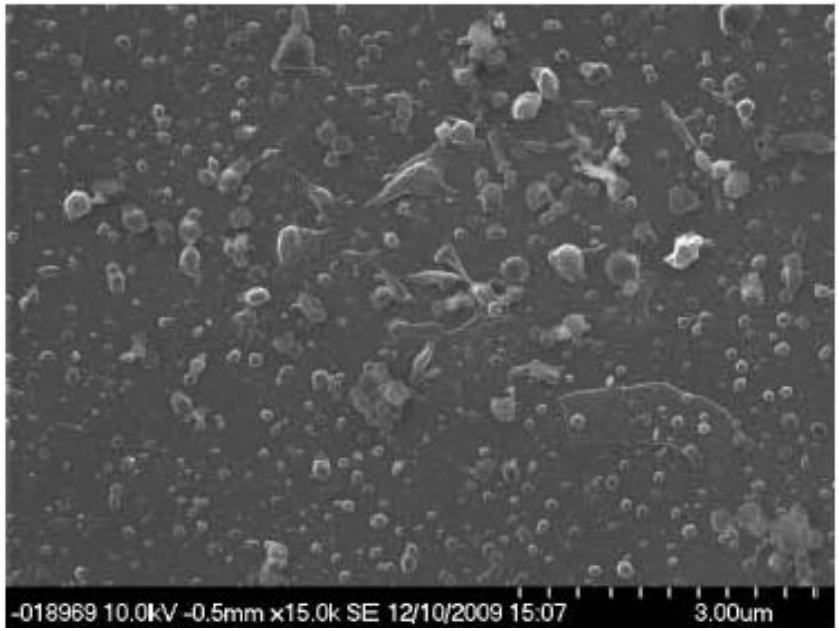
-018969 10.0kV -0.5mm x15.0k SE 12/10/2009 15:07
3.00um

F)

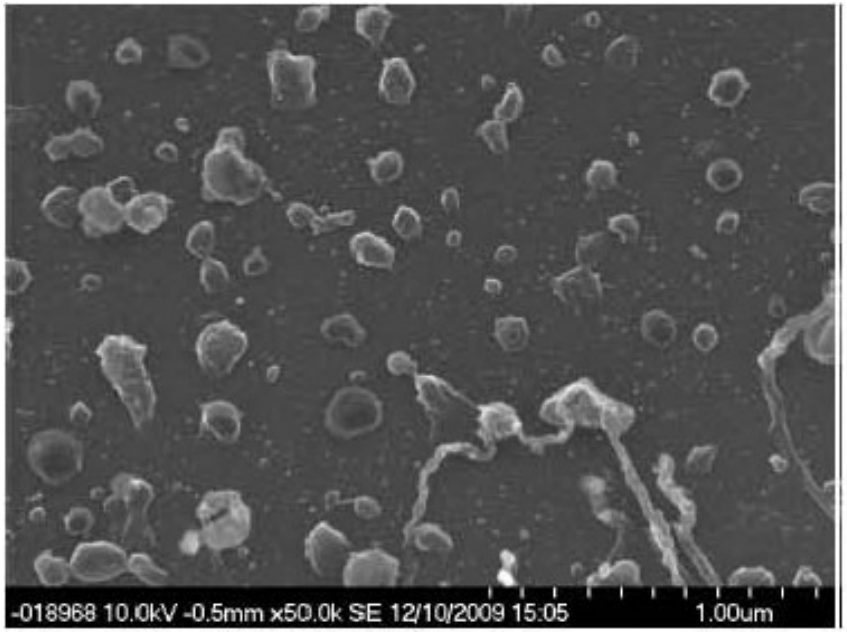
-018968 10.0kV -0.5mm x50.0k SE 12/10/2009 15:05
1.00um

G)

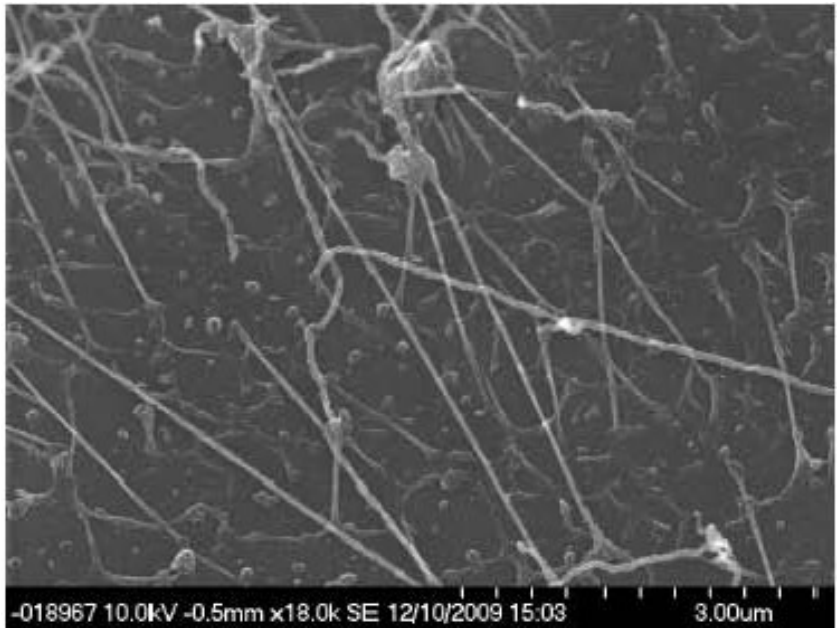
-018967 10.0kV -0.5mm x18.0k SE 12/10/2009 15:03
3.00um

H)

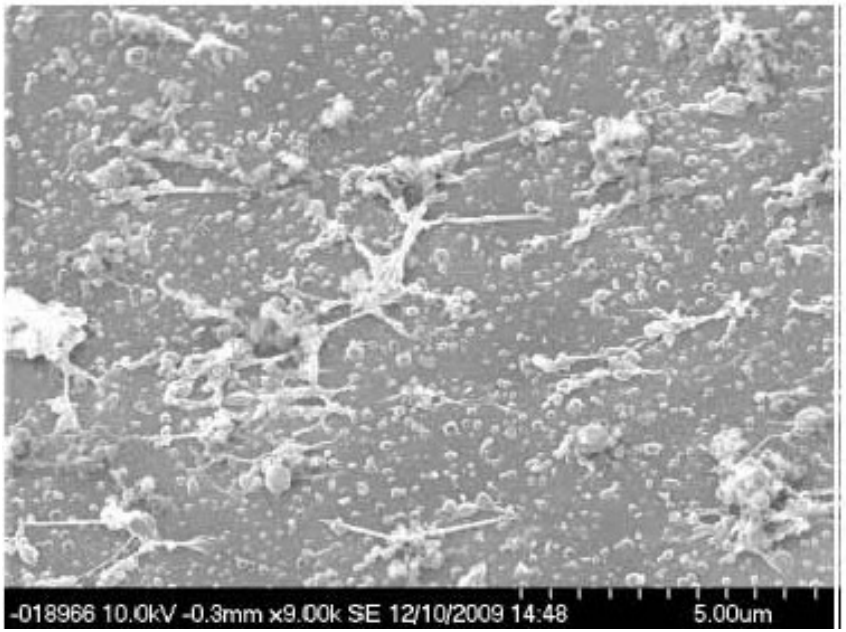
-018966 10.0kV -0.3mm x9.00k SE 12/10/2009 14:48
5.00um

Figure 10: SEM pictures of dER samples. All the pictures were taken at 10 kV. (A, B) SEM photograph of treatment 1 (Table 10) dER sample taken at x 15.000 and x11.000 magnification respectively from differing sites. Both show only vesicles of varying diameters (between 50 nm to 150 nm). The larger particles are aggregation of vesicles due to non-dispersion in 10% glycerol. Even larger aggregations (in the region of 0.5 to 3 µm) could be seen (data not shown). (C, D) SEM photographs of treatment 2 (Table 10) dER sample taken at x 13.000 magnification from differing sites. Both show vesicles of varying diameters. The larger particles are aggregations of vesicles due to non-dispersion in 10% glycerol. (E) SEM photograph of treatment 3 (Table 10)dER sample taken at x 15.000. Vesicles of varying diameters can be seen. Some particles with a structure different from vesicles can be discerned however, it can be noticed that these are largely drowned out by vesicles. No aggregates can be discerned. (F) SEM photographs of treatment 3 (Table 10) dER sample taken at x 50.000 magnification. This is a close-up of both vesicles and tubules in order to check for ribosomes, which are not present. The site photographed lies just outside (G). (G) SEM photograph of treatment 3 dER sample. Complex structures of tubular filaments connected to sheets can be discerned. The tubular filaments have a diameter of about 50-100 nm and are several µm long. It has to be taken into account that this is the only site where this structure was seen and was only discovered after scanning the chip for a long time. (H) SEM photograph of treatment 3 dER sample taken at x 9.000 magnification. Vesicles as well as complex structures can be seen. The vesicles are often attached to the complex structures (right bottom), giving the complex structures a more voluminous look. However it can be discerned that vesicles are far more numerous than complex structures and the complex structures do not seem as elaborate as in (G).

The SEM photographs taken while analysing samples of one standard dER preparation that have been treated differently before analysis (Table 10) can be seen in Figure 10.

The SEM photographs of dER sample that was not treated before drying for 24 hours (treatment 1) only show vesicles. Furthermore each sample was browsed for at least five minutes to see if the photographs taken are representative of the whole chip. It is important to note that the vesicles are of differing size (between <50 nm and 300 nm). The larger particles can be discerned as vesicle aggregation. These are due to the pelleting needed for ER isolation and the incomplete re-dispersion in 10% glycerol.

Larger vesicle aggregation could also be seen (ranging to a diameter of >3 μm) (data not shown), confirming that indeed the majority of the ER seen is in vesicular form.

The SEM photographs of dER sample that was not treated before drying but where the chip was coated with poly-lysine, which favors attachment of membranes proteins to the chip (treatment 2) also showed only vesicles of sizes similar as seen in the previous photographs. Some smaller vesicles aggregation can be discerned which hints at the ER preparation mostly consisting of vesicles.

The SEM photographs of dER sample that was treated with pre-fix before drying and was deposited on a poly-lysine coated chip show that indeed it consisted of a large number of vesicles (Figure 10, E and F), however some small complex structures can also be discerned. Although these are overshadowed in their membrane volume by the vesicles, it shows that some of the ER must have resisted the shearing forces of the ER preparation. The pre-fix contained para-formaldehyde and gluteraldehyde, both of which are cross-linking reagents and used extensively in electron microscopy because of their capacity to preserve complex structures [102-104].

Figure 10 (G) shows the site found where complex structures are more numerous than vesicles. Tubular filaments can be seen that are connected to sheet-like structures. The tubular filaments have a diameter of <50 nm and an overall length of several µm. If all the ER would still be in its complete state, then it could be expected to see a complicated mesh of tubular ER.

Figure 10 (H) shows a further site where some complex structure could be seen. These consist mainly of a few filaments of varying size. Vesicles can be seen to have aggregated around these complex structures indicating that the complex structures are surrounded by vesicles before re-suspension. It could be that these ultrastructures can be seen due to the difference in treatment of the sample. For the preparation of the sample pre-fix was used, which cross-links the proteins and therefore keeps the ultrastructure of the sample, however, in order to certify that these structures are present due to the adding of pre-fix, further samples need to be analysed. Due to time constraints, the author was not able to repeat the experiment.

3.3.3 Discussion

By closely looking at the SEM photographs of the ER samples, it can be concluded that the majority of the ER is present in a vesicular form. However a few complex structures could be observed.

The SEM used is the highest defining model that currently exists. Currently, no literature is available that looks at the structure of ER under an SEM, because, until the SEM that was used became available, no SEM had the resolution to see such fine structures. Although a TEM does have the required resolution, the fact that it can only look at small trans-section of the ER will only show an incomplete image of the ER. What would be seen mostly would be round spots, which may represent either the cross-section of a vesicle or of a tubule. This presents a problem with regard to identifying the complex structures that are visible in Figure 10 G).

As ribosomes can be detected at the magnifications used, these would provide evidence towards the nature of the complex structures seen. However, the method used for ER isolation involves the addition of EDTA to the homogenization buffer as well as to the sucrose gradients. This has as effect to release the ribosomes from ER, hence prohibiting identification of the complex structures as ER. Martin Goldberg (Goldberg, unpublished) analysed a preparation of chicken ER (Figure 11), which, given the circumstances, represents the closest comparison to plant ER available. The ribosomes can still be discerned on the sheets and tubules, hence identifying the structures seen as ER.

Although differences between the chicken ER and the complex structures (Figure 10, G) can be seen, the complex structures also consist of sheets and tubules of approximately the same size. The main difference is that the complex structures have far longer tubules and smaller sheets.

Taking into consideration that two ER preparation from hosts of different kingdoms are compared, it can be concluded that the complex structures observed in Figure 10 G) are indeed ER.

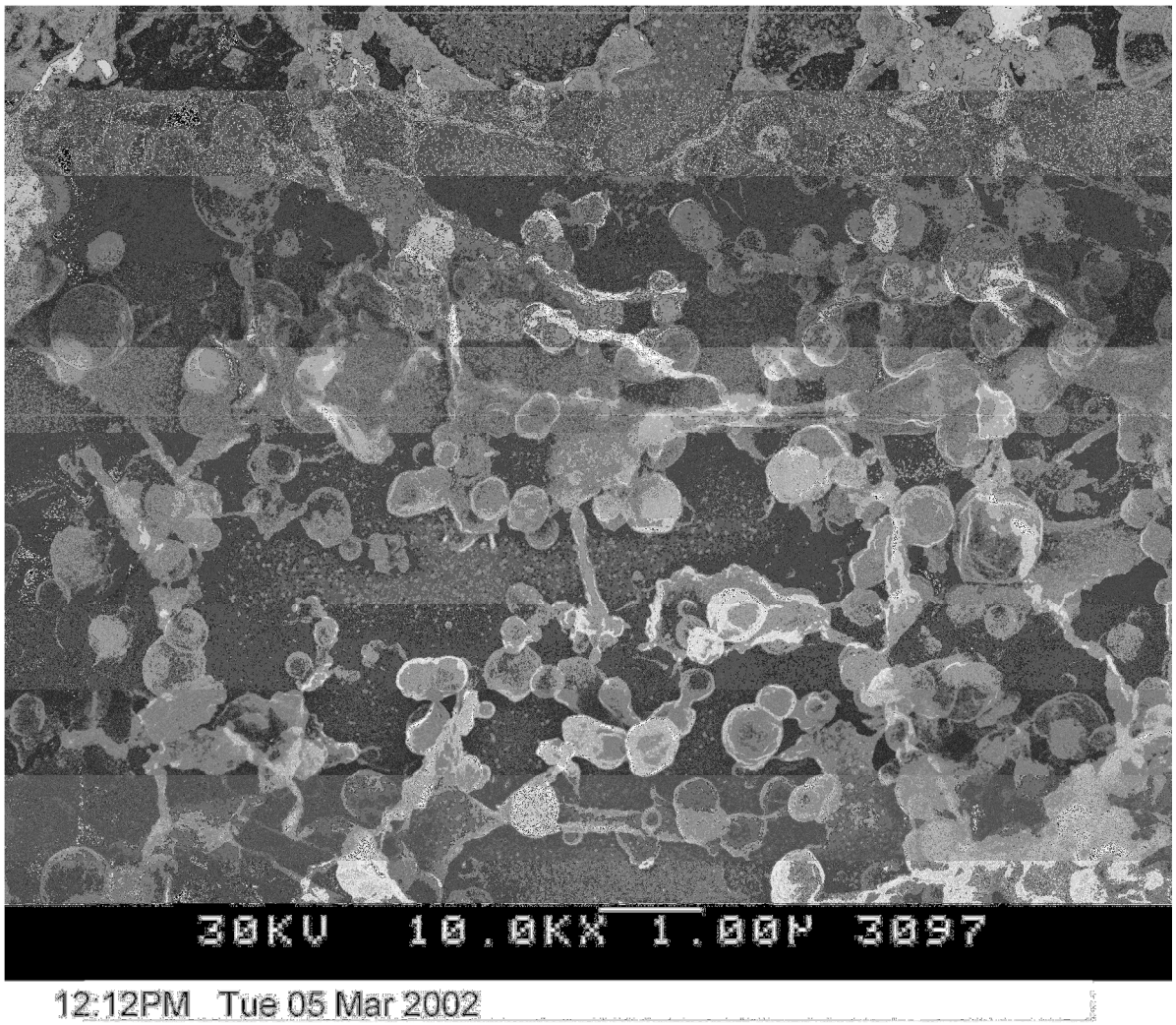

Figure 11: SEM photograph of chicken ER at a magnification of x 10.000 and 30 kV. A mixture of tubules, sheets and vesicle can be seen. The tubules and sheets still show ribosomes. These are so large that they can still be seen as speckles. This indicates that the sample seen is indeed ER [101].

The sample preparation included letting the dER preparation stand for 24 hours at 4°C, as well as drying. During this process, it could be possible that the membranes lysed and formed vesicles. In order to control for this, dER that has been treated with pre-fix, which contains gluteraldehyde as well as para-formaldehyde. The pre-fix crosslinks the proteins in the sample, thereby immobilizing them in their present form. The drying process will not have influenced the shape of this dER sample [104]. The SEM photograph shows exactly the same prevalence of vesicles as the two other treated samples. However, it has to be noted that indeed more complex structures can be observed in the pre-fix treated sample than in the other two samples. However, the vesicles far outnumber the complex structures in all of the samples.

Theoretically, whole ER may not have attached to the silicon chip as well as vesicles, therefore may have been washed off during the washing or drying steps. However, the presence of very large aggregates of vesicles (which represent part of the non-dispersed pellet) indicate that vesicles are far more prevalent than whole ER. Furthermore, out of the three chips analysed, only one small site could be identified where whole ER outnumbered vesicles. In other parts only small complex structures could be seen. These showed either tubules or sheets and not, like in Figure 10 G), both. However, the possibility of a "stickiness" difference exists, although it can be assumed that the majority of the ER is present in the form of vesicles. As already determined in the introduction to this chapter, once membranes are ruptured (as they need to be in order to form vesicles), membranes can close, with equal probability, either the right way or the wrong way around. This would significantly hinder membrane topology elucidation, since the experiment cannot determine the sidedness of proteins using a mixture of flipped and unflipped membranes.

Further experiments, which are not within the scope of this thesis, need to be done in order to determine the exact ratio of flipped and non-flipped membranes. It would be possible to

determine sidedness by raising 2 different types of antibodies using peptides from either the cytosolic or lumenar part of an IMP and labelled with either Cy-3 or Cy-5. The outside of the ER would then have to be shaved using a protease. By then comparing the relative amounts of both antibodies to a Ricinus developing seed homogenate (tagged with both Cy-3 and Cy-5), it will be possible to determine the exact ratio of flipped and non-flipped membranes.

4. Conclusion

A comparison between predicted ER localised proteins (in Arabidopsis) [65, 67] and ER proteins of *Ricinus communis* [2] should allow the identification of proteins that may be involved in storage lipid production. In a comparison of Ricinus ER proteins and the Ricinus equivalent of Arabidopsis predicted ER proteins [65, 67] showed that 133 protein homologs overlapped with the MudPIT data and 95 did not.

A comparison the other way (Arabidopsis homologs of Ricinus ER proteins, as identified in the MudPIT experiment, against the Arabidopsis tissue culture LOPIT predicted-ER data) showed that 220 were not present in the Arabidopsis tissue culture LOPIT data. The function gene ontology of these was then searched in the Uniprot database. 5 proteins could be identified that were localised in the ER and were involved in lipid synthesis, fatty acid biosynthesis and triacylglycerol assimilation. These were 3β- hydroxysteroid-dehydrogenase, 3-oxoacyl-ACP reductase, FAD2, a lipase class 3 family protein and a diacylglycerol acyltransferase family. Further search in different databases revealed that 3β-hydroxysteroid-dehydrogenase is involved in sterol production and was wrongly classified, that 3-oxoacyl-ACP reductase is another name for βKR, that FAD2 is a well known enzyme in storage lipid biosynthesis, that a lipase is involved in storage lipid breakdown and that the DGAT family protein is already known to the authors lab (unpublished data) to be involved in storage lipid production in seeds in Ricinus. It can be concluded that a comparison between predicted ER proteins in Arabidopsis and ER proteins in Ricinus does not allow the identification of yet unknown proteins that are involved in the biosynthesis of fatty acids.

A further contamination gene ontology search showed that the ER prep does contain some contamination of proteins from other organelles and the cytoplasm (Appendix A). It has to be noted that the mass spectrometry detection method used does not allow the quantification of the contamination. By detecting the contamining proteins, it will be possible to use Western blotting followed by Cy-3 secondary antibody detection to quantify select contaminating proteins.

A western blotting analysis of chosen contaminating marker proteins was performed, using Cy-3 conjugated secondary antibodies. The use of Cy-3 conjugated secondary antibodies allowed the relative quantification of the contaminants in the ER prep as compared to homogenated developing seed. Only a subset of mitochondrial proteins could be identified in the *Ricinus communis* MudPIT ER analysis [2]. The identification of these proteins however is not conclusive to whole mitochondria co-purifying alongside the ER. At an enrichment of 5x, the mass spectrometer would have identified further mitochondrial proteins. The lack of further identified mitochondrial marker at a 5x enrichment as compared to developing seed homogenate, suggest strongly that the contamination consists of single proteins co-purifying together with ER and not whole mitochondria. From the aspect of contamination, an ER membrane topology experiment would be feasible. A further AQUA analysis, as according to Gerber et al. [105] would be needed to absolutely quantify the contamination of ER preparations.

A SEM study of an ER prep was then done. Three different methods were investigated to enable the fixation of ER to the silicon chip and enable microscopy analysis. All three showed that the ER prep consists of a majority of vesicles. Considering that vesicles primarily form due to rupturing of membranes, and that membranes tend to close either way around when ruptured, it can be assumed that a high percentage of the membranes show the lumenar side of the membrane to the exterior. Hence all membrane topology would be lost [106].

Although the SEM analysis of the ER prep does not prove the sidedness of the membrane, it gives a picture of the state of ER organelles. Considering the thermodynamic properties of membranes, the presence of vesicles indicates that the membranes have been ruptured at some point during the preparation. Therefore it can be assumed that the standard ER-preparation analysed, prepared according to the method by Simon et al. [2], does not meet all the criteria necessary for membrane topology elucidation. A membrane topology elucidation does not seem feasible using ER purified according to the method determined by Simon et al. [2]. This stands in contrast to claims by Simon et. al who state that the purified ER is whole [2].

Furthermore, it can be concluded that although an ER enrichment does occur, the preparation is not free of contamination (as would be expected). However, none of these contaminations are due to whole mitochondria co-purifying alongside ER.

The ER preparation as according to Simon et al. [2] does not seem to purify ER as whole organelles but rather as vesicles. The membrane topology does not seem conserved during preparation, hence a membrane topology elucidation experiment is not feasible. Such a preparation would be extremely useful when analyzing membrane proteins.

Appendix A

Accession nr	Accession nr Ara	ER	Plasma membrane	Golgi Apparatus	Vacuole	Chloroplast	Mitochondria	Peroxysome	Cytoplasm	Integral to membrane	Nuclear envelope	Others
29682.m000596	AT5G46850.1	X										
29739.m003645	AT2G26260.1	X										
29851.m002399	AT4G04955.1	X										
29950.m001177	AT5G18290.1	X										
30204.m001732	AT5G48660.1	X										
29676.m001644	AT2G23640.1	X										
30076.m004672	AT4G02080.1	X	X	X								
30005.m001286	AT4G08810.1	X									X	
30076.m004681	AT3G62600.1	X	X									
30169.m006262	AT1G50430.1	X	X									
29727.m000478	AT1G11890.1	X	X	X								
28469.m000076	AT4G27500.1	X			X							
28401.m000076	AT5G48580.1	X			X							
27940.m000340	AT4G17050.1											
30128.m008763	AT1G54860.1											Anchored to membrane
29887.m000234	AT5G02500.1		x	x	x							
30025.m000589	AT5G02500.1		x	x	x							
29585.m000574	AT5G02500.1		x	x	x	x	x					
29751.m001894	AT3G46740.1					x						
30142.m000636	AT4G35860.1					x						
27394.m000344	AT1G15690.1		x	x	x	x	x					
30170.m013972	AT5G42650.1					x						
39369.m000014	AT4G13010.1		x		x	x						
30120.m000353	AT4G13010.1		x		x	x						

30293.m000014	AT4G13010.1		x		x	x						
29929.m004594	AT2G27490.2				x	x						
30170.m014016	AT5G42960.1					x	x					
29822.m003473	AT3G01280.1		x		x	x	x					
29602.m000217	AT4G35000.1		x		x	x	x	x				
29736.m002034	AT3G01280.1		x		x	x	x					
30131.m006881	AT1G16030.1		x			x						
30131.m006880	AT1G16030.1		x			x						
30190.m010783	AT4G11150.1		x		x				x			
29836.m000559	AT5G09810.1		x						x			Cytoskeleton
30003.m000328	AT3G46520.1		x						x			Cytoskeleton
29686.m000868	AT3G12490.1											Extracellular
29822.m003420	AT5G14950.1			x								
30170.m014160	AT3G27230.1			x								
30076.m004636	AT3G66654.1		x	x								
27732.m000289	AT1G09580.1									x		
29792.m000626	AT3G26320.1									x		
29780.m001395	AT1G68100.1									x		
30169.m006444	AT3G20920.1									x		
30138.m004002	AT5G07920.1									x		
29889.m003283	AT3G17000.1									x		
30128.m008768	AT3G63150.1						x					
30170.m013947	AT1G47640.1						x					
29889.m003274	AT4G16160.2						x					
30154.m001133	AT5G24650.1		x		x	x	x					
29613.m000365	AT3G46520.1						x					Cytoskeleton
29917.m001992	AT3G01570.1											Lipid storage body
30147.m014333	AT4G25140.1											Lipid storage body
30138.m004021	AT4G00050.1										x	
30174.m008963	AT1G01820.1							x				

30147.m013773	AT5G03860.1							x				
30170.m014001	AT1G47750.1							x				
30156.m001743	AT3G21865.1							x				
30131.m007005	AT5G14030.1		x									
29782.m000120	AT3G51050.1		x									
29200.m000172	AT1G04430.2		x	x								
29602.m000216	AT2G20990.1		x		x							
30174.m008919	AT3G61050.1		x									
28320.m001115	AT3G57340.2		x									
28449.m000019	AT5G59840.1		x									
30131.m007265	AT5G08580.1		x									
29671.m000296	AT4G29960.1		x									
29830.m001439	AT3G51460.1		x									
30131.m007267	AT3G20000.1		x			x	x					
30190.m011126	AT1G12640.1		x		x							
28629.m000567	AT3G52590.1		x		x							
29631.m001047	AT2G47110.1		x		x							
30000.m000379	AT3G52590.1		x		x							
30076.m004585	AT2G47110.1		x		x							
30169.m006323	AT1G31340.1		x		x							
29864.m001484	AT3G21640.1		x		x							
29805.m001531	AT4G17170.1		x		x							
28623.m000398	AT1G75630.1		x		x							
29908.m006129	AT1G75630.1		x		x							
30131.m007140	AT2G16510.1		x		x							
29912.m005437	AT4G29130.1		x		x	x	x				x	
30206.m000761	AT5G09810.1		x									Cytoskeleton
29739.m003689	AT1G53920.1											
29662.m000463	AT5G20500.1											Secreted
30183.m001284	AT2G31980.1											Secreted
30169.m006261	AT1G78900.2				x							

29681.m001366	AT1G17810.1				x							
27516.m000171	AT5G20660.1				x							
27516.m000171	AT5G20660.1				x							
30170.m014224	AT1G19910.1		x		x							

5. Bibliography

[1] Brockerhoff, H., Stereospecific analysis of triglycerides. Lipids 1971, 6, 942-956.

[2] Simon, W., Maltman, D., Slabas, A., Isolation and Fractionation of the Endoplasmic Reticulum from Castor Bean (*Ricinus communis*) Endosperm for Proteomic Analyses. METHODS IN MOLECULAR BIOLOGY-CLIFTON THEN TOTOWA- 2008, 425, 203.

[3] Knutzon, D., Thompson, G., Radke, S., Johnson, W., et al., Modification of Brassica seed oil by antisense expression of a stearoyl-acyl carrier protein desaturase gene. Proceedings of the National Academy of Sciences 1992, 89, 2624.

[4] Gunstone, F., Wijesundera, R., Fatty acids, part 54. Some reactions of long-chain oxygenated acids with special reference to those furnishing furanoid acids* 1. Chemistry and Physics of Lipids 1979, 24, 193-208.

[5] Ichihara, K., sn-Glycerol-3-phosphate acyltransferase in a particulate fraction from maturing safflower seeds. Archives of Biochemistry and Biophysics 1984, 232, 685-698.

[6] Murphy, D., Production of novel oils in plants. Current Opinion in Biotechnology 1999, 10, 175-180.

[7] Caupin, H., Products from castor oil: past, present, and future. Lipid Technologies and Applications 1997, 787–795.

[8] Caupin, H. j., Lipid technologies and Application. Technology and Engineering 1997.

[9] McKeon, T., Engineering Plants for Industrial Uses. Biocatalysis and Agricultural Biotechnology 2009, 89.

[10] Frewer, L., Howard, C., Shepherd, R., Public concerns in the United Kingdom about general and specific applications of genetic engineering: Risk, benefit, and ethics. Science, technology & human values 1997, 22, 98.

[11] Hails, R., Genetically modified plants-the debate continues. Trends in Ecology & Evolution 2000, 15, 14-18.

[12] Rudloff, E., Wehling, P., ISHS 1997, pp. 379-388.

[13] Murphy, D., Vance, J., Mechanisms of lipid-body formation. Trends in biochemical sciences 1999, 24, 109-115.

[14] Daum, G., Wagner, A., Czabany, T., Athenstaedt, K., Dynamics of neutral lipid storage and mobilization in yeast. Biochimie 2007, 89, 243-248.

[15] Sasaki, Y., Nagano, Y., Plant acetyl-CoA carboxylase: structure, biosynthesis, regulation, and gene manipulation for plant breeding. Bioscience, biotechnology, and biochemistry 2004, 68, 1175-1184.

[16] Smith, S., The animal fatty acid synthase: one gene, one polypeptide, seven enzymes. The FASEB Journal 1994, 8, 1248.

[17] Slabas, A., Hanley, Z., Schierer, T., Rice, D., et al., Acyltransferases and their role in the biosynthesis of lipids-opportunities for new oils. Journal of Plant Physiology 2001, 158, 505-513.

[18] Salas, J., Sánchez, J., Ramli, U., Manaf, A., et al., Biochemistry of lipid metabolism in olive and other oil fruits. Progress in Lipid Research 2000, 39, 151-180.

[19] Gadd, S., School of Biological and Biomedial Sciences, Durham University 2009, p. 307.

[20] Koo, A., Ohlrogge, J., Pollard, M., On the export of fatty acids from the chloroplast. Journal of Biological Chemistry 2004, 279, 16101.
[21] Bates, P., Ohlrogge, J., Pollard, M., Incorporation of newly synthesized fatty acids into cytosolic glycerolipids in pea leaves occurs via acyl editing. Journal of Biological Chemistry 2007, 282, 31206.
[22] Hellyer, A., Leadlay, P., Slabas, A., Induction, purification and characterisation of acyl-ACP thioesterase from developing seeds of oil seed rape (Brassica napus). Plant molecular biology 1992, 20, 763-780.
[23] Shanklin, J., Somerville, C., Stearoyl-acyl-carrier-protein desaturase from higher plants is structurally unrelated to the animal and fungal homologs. Proc. Natl. Acad. Sci. USA 1991, 88, 2510-2514.
[24] Harwood, J., Recent advances in the biosynthesis of plant fatty acids. Biochimica et Biophysica Acta (BBA)/Lipids and Lipid Metabolism 1996, 1301, 7-56.
[25] Morris, L., The mechanism of ricinoleic acid biosynthesis in Ricinus communis seeds. Biochemical and biophysical research communications 1967, 29, 311.
[26] Maltman, D., Simon, W., Wheeler, C., Dunn, M., et al., Proteomic analysis of the endoplasmic reticulum from developing and germinating seed of castor(*Ricinus communis*). Electrophoresis 2002, 23, 626.
[27] BAFOR, M., SMITH, M., t Lisbeth JONSSON, K., STYMNE, S., Ricinoleic acid biosynthesis and triacylglycerol assembly in microsomal preparations from developing castor-bean. Biochem. J 1991, 280, 507-514.
[28] McKeon, T., Chen, G., Lin, J., Biochemical aspects of castor oil biosynthesis. BIOCHEMICAL SOCIETY TRANSACTIONS 2000, 28, 972-973.
[29] Van de Loo, F., Broun, P., Turner, S., Somerville, C., An oleate 12-hydroxylase from *Ricinus communis* L. is a fatty acyl desaturase homolog. Proceedings of the National Academy of Sciences 1995, 92, 6743.
[30] Broun, P., Somerville, C., Accumulation of Ricinoleic, Lesquerolic, and Densipolic Acids in Seeds of Transgenic Arabidopsis Plants That Express a Fatty Acyl Hydroxylase cDNA from Castor Bean. American Society Plant Biology 1997, 113, 933-942.
[31] Domergue, F., Chevalier, S., Créach, A., Cassagne, C., Lessiré, R., Purification of the acyl-CoA elongase complex from developing rapeseed and characterization of the 3-ketoacyl-CoA synthase and the 3-hydroxyacyl-CoA dehydratase. Lipids 2000, 35, 487-494.
[32] Alberts, B. J., A; Lewis, J; Raff, M; Roberts, K; Walter, P (Ed.), Molecular Biology of the Cell, 2008.
[33] Kennedy, E., Lehninger, A., Oxidation of fatty acids and tricarboxylic acid cycle intermediates by isolated rat liver mitochondria. Journal of Biological Chemistry 1949, 179, 957.
[34] Kennedy, E., Weiss, S., The function of cytidine coenzymes in the biosynthesis of phospholipides. Journal of Biological Chemistry 1956, 222, 193.
[35] Zheng, Z., Xia, Q., Dauk, M., Shen, W., et al., Arabidopsis AtGPAT1, a member of the membrane-bound glycerol-3-phosphate acyltransferase gene family, is essential for tapetum differentiation and male fertility. The Plant Cell Online 2003, 15, 1872.
[36] Cao, Y., Oo, K., Huang, A., Lysophosphatidate acyltransferase in the microsomes from maturing seeds of meadowfoam (Limnanthes alba). Plant Physiology 1990, 94, 1199.
[37] Brown, A., Brough, C., Kroon, J., Slabas, A., Identification of a cDNA that encodes a 1-acyl-sn-glycerol-3-phosphate acyltransferase from Limnanthes douglasii. Plant molecular biology 1995, 29, 267-278.

[38] Kim, H., Li, Y., Huang, A., Ubiquitous and endoplasmic reticulum-located lysophosphatidyl acyltransferase, LPAT2, is essential for female but not male gametophyte development in Arabidopsis. The Plant Cell Online 2005, 17, 1073.
[39] Kates, M., Hydrolysis of lecithin by plant plastid enzymes. Biochemistry and Cell Biology 1955, 33, 575-589.
[40] Pearce, M., Slabas, A., Phosphatidate phosphatase from avocado (Persea americana)-purification, substrate specificity and possible metabolic implications for the Kennedy pathway and cell signalling in plants. The Plant Journal 1998, 14, 555-564.
[41] Pierrugues, O., Brutesco, C., Oshiro, J., Gouy, M., et al., Lipid phosphate phosphatases in Arabidopsis. Regulation of the AtLPP1 gene in response to stress. Journal of Biological Chemistry 2001, 276, 20300.
[42] Nakamura, Y., Tsuchiya, M., Ohta, H., Plastidic phosphatidic acid phosphatases identified in a distinct subfamily of lipid phosphate phosphatases with prokaryotic origin. Journal of Biological Chemistry 2007, 282, 29013.
[43] França, M., Matos, A., D'arcy-Lameta, A., Passaquet, C., et al., Cloning and characterization of drought-stimulated phosphatidic acid phosphatase genes from Vigna unguiculata. Plant Physiology and Biochemistry 2008, 46, 1093-1100.
[44] Dauk, M., Lam, P., Smith, M., The role of diacylglycerol acyltransferase-1 and phospholipid: diacylglycerol acyltransferase-1 and-2 in the incorporation of hydroxy fatty acids into triacylglycerol in Arabidopsis thaliana expressing a castor bean oleate 12-hydroxylase gene. Botany 2009, 87, 552-560.
[45] Dahlqvist, A., Ståhl, U., Lenman, M., Banas, A., et al., Phospholipid: diacylglycerol acyltransferase: an enzyme that catalyzes the acyl-CoA-independent formation of triacylglycerol in yeast and plants. Proceedings of the National Academy of Sciences of the United States of America 2000, 97, 6487.
[46] Hobbs, D., Lu, C., Hills, M., Cloning of a cDNA encoding diacylglycerol acyltransferase from Arabidopsis thaliana and its functional expression. FEBS letters 1999, 452, 145-149.
[47] He, X., Turner, C., Chen, G., Lin, J., McKeon, T., Cloning and characterization of a cDNA encoding diacylglycerol acyltransferase from castor bean. Lipids 2004, 39, 311-318.
[48] Jako, C., Kumar, A., Wei, Y., Zou, J., et al., Seed-specific over-expression of an Arabidopsis cDNA encoding a diacylglycerol acyltransferase enhances seed oil content and seed weight. Plant Physiology 2001, 126, 861.
[49] Mhaske, V., Beldjilali, K., Ohlrogge, J., Pollard, M., Isolation and characterization of an Arabidopsis thaliana knockout line for phospholipid: diacylglycerol transacylase gene (At5g13640). Plant Physiology and Biochemistry 2005, 43, 413-417.
[50] Stahl, U., Carlsson, A., Lenman, M., Dahlqvist, A., et al., Cloning and functional characterization of a phospholipid: diacylglycerol acyltransferase from Arabidopsis. Plant Physiology 2004, 135, 1324.
[51] Ramli, U., Salas, J., Quant, P., Harwood, J., Metabolic control analysis reveals an important role for diacylglycerol acyltransferase in olive but not in oil palm lipid accumulation. FEBS JOURNAL 2005, 272, 5764.
[52] Cases, S., Stone, S., Zhou, P., Yen, E., et al., Cloning of DGAT2, a second mammalian diacylglycerol acyltransferase, and related family members. Journal of Biological Chemistry 2001, 276, 38870.
[53] Stone, S., Myers, H., Watkins, S., Brown, B., et al., Lipopenia and skin barrier abnormalities in DGAT2-deficient mice. Journal of Biological Chemistry 2004, 279, 11767.
[54] Kroon, J., Wei, W., Simon, W., Slabas, A., Identification and functional expression of a type 2 acyl-CoA: diacylglycerol acyltransferase (DGAT2) in developing castor bean seeds which has

high homology to the major triglyceride biosynthetic enzyme of fungi and animals. Phytochemistry 2006, 67, 2541-2549.
[55] Burgal, J., Shockey, J., Lu, C., Dyer, J., et al., Metabolic engineering of hydroxy fatty acid production in plants: RcDGAT2 drives dramatic increases in ricinoleate levels in seed oil. Plant biotechnology journal 2008, 6, 819-831.
[56] Lacey, D., Hills, M., Heterogeneity of the endoplasmic reticulum with respect to lipid synthesis in developing seeds of Brassica napus L. Planta 1996, 199, 545-551.
[57] Fraser, T., Waters, A., Chatrattanakunchai, S., Stobart, K., Does triacylglycerol biosynthesis require diacylglycerol acyltransferase (DAGAT)? BIOCHEMICAL SOCIETY TRANSACTIONS 2000, 28, 698-700.
[58] Napier, J., The production of unusual fatty acids in transgenic plants. 2007.
[59] Righetti, P., Stoyanov, A., Zhukov, M., The Proteome Revisited: Theory and Practice of All Relevant Electrophoretic Steps, Elsevier Science 2001.
[60] Cao, B., Porollo, A., Adamczak, R., Jarrell, M., Meller, J., Enhanced recognition of protein transmembrane domains with prediction-based structural profiles. Bioinformatics 2006, 22, 303-309.
[61] Kagawa, T., Lord, J., Beevers, H., The Origin and Turnover of Organelle Membranes in Castor Bean Endosperm 1. Plant Physiology 1973, 51, 61-65.
[62] Lord, J., Kagawa, T., Moore, T., Beevers, H., Endoplasmic reticulum as the site of lecithin information in castor bean endosperm. The Journal of Cell Biology 1973, 57, 659-667.
[63] Moore, T., Lord, J., Kagawa, T., Beevers, H., Enzymes of Phospholipid Metabolism in the Endoplasmic Reticulum of Castor Bean Endosperm 1. Plant Physiology 1973, 52, 50-53.
[64] Coughlan, S., Hastings, C., Winfrey, R., Identification of Protein Disulfide-Isomerase as the Major Reticuloplasmin. European Journal of Biochemistry 1996, 235, 215-224.
[65] Dunkley, T., Watson, R., Griffin, J., Dupree, P., Lilley, K., Localization of Organelle Proteins by Isotope Tagging (LOPIT)* S. Molecular & Cellular Proteomics 2004, 3, 1128-1134.
[66] Ford, T., Graham, J., Rickwood, D., Iodixanol: A Nonionic Iso-osmotic Centrifugation Medium for the Formation of Self-Generated Gradients. Analytical Biochemistry 1994, 220, 360-366.
[67] Dunkley, T., Hester, S., Shadforth, I., Runions, J., et al., Mapping the Arabidopsis organelle proteome. Proceedings of the National Academy of Sciences 2006, 103, 6518-6523.
[68] Chen, X., Ulintz, P. J., Simon, E. S., Williams, J. A., Andrews, P. C., Global topology analysis of pancreatic zymogen granule membrane proteins. Mol Cell Proteomics 2008.
[69] Crystal, A. S., Morais, V. A., Pierson, T. C., Pijak, D. S., et al., Membrane topology of gamma-secretase component PEN-2. J Biol Chem 2003, 278, 20117-20123.
[70] Feramisco, J. D., Goldstein, J. L., Brown, M. S., Membrane topology of human insig-1, a protein regulator of lipid synthesis. J Biol Chem 2004, 279, 8487-8496.
[71] Wu, C., MacCoss, M., Howell, K., Yates, J., A method for the comprehensive proteomic analysis of membrane proteins. Nature Biotechnology 2003, 21, 532-538.
[72] Wu, C., Yates, J., The application of mass spectrometry to membrane proteomics. Nature Biotechnology 2003, 21, 262-267.
[73] Steinberg, T., Jones, L., Haugland, R., Singer, V., SYPRO orange and SYPRO red protein gel stains: one-step fluorescent staining of denaturing gels for detection of nanogram levels of protein. Analytical Biochemistry 1996, 239, 223-237.
[74] Yen, C., Stone, S., Koliwad, S., Harris, C., Farese Jr, R., Thematic review series: glycerolipids. DGAT enzymes and triacylglycerol biosynthesis. The Journal of Lipid Research 2008, 49, 2283.
[75] Ichihara, K., Takahashi, T., Fujii, S., Diacylglycerol acyltransferase in maturing safflower seeds: its influences on the fatty acid composition of triacylglycerol and on the rate of

triacylglycerol synthesis. Biochimica et Biophysica Acta (BBA)-Lipids and Lipid Metabolism 1988, 958, 125-129.
[76] Katavic, V., Reed, D., Taylor, D., Giblin, E., et al., Alteration of seed fatty acid composition by an ethyl methanesulfonate-induced mutation in Arabidopsis thaliana affecting diacylglycerol acyltransferase activity. Plant Physiology 1995, 108, 399.
[77] Vogel, G., Cholinephosphotransferase and Diacylglycerol Acyltransferase (Substrate Specificities at a Key Branch Point in Seed Lipid Metabolism). Plant Physiology 1996, 110, 923.
[78] Lin, J., Woodruff, C., Lagouche, O., McKeon, T., et al., Biosynthesis of triacylglycerols containing ricinoleate in castor microsomes using 1-acyl-2-oleoyl-sn-glycero-3-phosphocholine as the substrate of oleoyl-12-hydroxylase. Lipids 1998, 33, 59-69.
[79] Smith, M., Moon, H., Chowrira, G., Kunst, L., Heterologous expression of a fatty acid hydroxylase gene in developing seeds of Arabidopsis thaliana. Planta 2003, 217, 507-516.
[80] Lu, C., Fulda, M., Wallis, J., A high-throughput screen for genes from castor that boost hydroxy fatty acid accumulation in seed oils of transgenic Arabidopsis. The Plant Journal 2006, 45, 847-856.
[81] Kumar, R., Wallis, J., Skidmore, C., A mutation in Arabidopsis cytochrome b5 reductase identified by high-throughput screening differentially affects hydroxylation and desaturation. The Plant Journal 2006, 48, 920-932.
[82] Emanuelsson, O., Nielsen, H., Brunak, S., von Heijne, G., Predicting subcellular localization of proteins based on their N-terminal amino acid sequence. Journal of Molecular Biology 2000, 300, 1005-1016.
[83] Schwacke, R., Schneider, A., van der Graaff, E., Fischer, K., et al., ARAMEMNON, a novel database for Arabidopsis integral membrane proteins. Plant Physiology 2003, 131, 16.
[84] Rahier, A., Darnet, S., Bouvier, F., Camara, B., Bard, M., Molecular and enzymatic characterizations of novel bifunctional 3beta-hydroxysteroid dehydrogenases/C-4 decarboxylases from Arabidopsis thaliana. Journal of Biological Chemistry 2006, 281, 27264.
[85] Sheldon, P., Kekwick, R., Sidebottom, C., Smith, C., Slabas, A., 3-Oxoacyl-(acyl-carrier protein) reductase from avocado (Persea americana) fruit mesocarp. Biochemical Journal 1990, 271, 713.
[86] Lin, Y., Wimer, L., Huang, A., Lipase in the lipid bodies of corn scutella during seedling growth. Plant Physiology 1983, 73, 460.
[87] Maeshima, M., Beevers, H., Purification and properties of glyoxysomal lipase from castor bean. Plant Physiology 1985, 79, 489.
[88] Eastmond, P., Cloning and characterization of the acid lipase from castor beans. Journal of Biological Chemistry 2004, 279, 45540.
[89] Howell, K., Devaney, E., Gruenberg, J., Subcellular fractionation of tissue culture cells. Trends in biochemical sciences 1989, 14, 44.
[90] Pasquali, C., Fialka, I., Huber, L., Subcellular fractionation, electromigration analysis and mapping of organelles. Journal of Chromatography B: Biomedical Sciences and Applications 1999, 722, 89-102.
[91] Huber, L., Pfaller, K., Vietor, I., Organelle proteomics: implications for subcellular fractionation in proteomics. Circulation research 2003, 92, 962.
[92] Schutz-Geschwender, A., Zhang, Y., Holt, T., McDermitt, D., Olive, D., Quantitative, two-color Western blot detection with infrared fluorescence. LI-COR Biosciences 2004.
[93] Clausen, C., Ilkavets, I., Thomson, R., Philippar, K., et al., Intracellular localization of VDAC proteins in plants. Planta 2004, 220, 30-37.
[94] Mullen, R., Trelease, R., The ER-peroxisome connection in plants: development of the" ER semi-autonomous peroxisome maturation and replication" model for plant peroxisome biogenesis. Biochimica Et Biophysica Acta-Molecular Cell Research 2006, 1763, 1655-1668.

[95] Schluter, A., Fourcade, S., Ripp, R., Mandel, J., et al., The evolutionary origin of peroxisomes: an ER-peroxisome connection. Molecular biology and evolution 2006, 23, 838.
[96] Titorenko, V., Mullen, R., Peroxisome biogenesis: the peroxisomal endomembrane system and the role of the ER. Journal of Cell Biology 2006, 174, 11.
[97] Millar, A., Sweetlove, L., Giege, P., Leaver, C., Analysis of the Arabidopsis mitochondrial proteome. Plant Physiology 2001, 127, 1711.
[98] Kruft, V., Eubel, H., Jansch, L., Werhahn, W., Braun, H., Proteomic approach to identify novel mitochondrial proteins in Arabidopsis. Plant Physiology 2001, 127, 1694.
[99] Goldstein, J., Newbury, D., Echlin, P., Lyman, C., et al., Scanning electron microscopy and X-ray microanalysis, Plenum Pub Corp 2003.
[100] Oatley, The scanning electron microscope, Cambridge University press 1972.
[101] English, A., Zurek, N., Voeltz, G., Peripheral ER structure and function. Current opinion in cell biology 2009, 21, 596-602.
[102] McLEAN, I., NAKANE, P., Periodate-lysine-paraformaldehyde fixative a new fixative for immunoelectron microscopy. Journal of Histochemistry and Cytochemistry 1974, 22, 1077.
[103] Grimaud, J., Druguet, M., Peyrol, S., Chevalier, O., et al., Collagen immunotyping in human liver: light and electron microscope study. Journal of Histochemistry and Cytochemistry 1980, 28, 1145.
[104] Iliescu, M., Hoemann, C., Shive, M., Chenite, A., Buschmann, M., Ultrastructure of hybrid chitosan-glycerol phosphate blood clots by environmental scanning electron microscopy. Microscopy research and technique 2008, 71, 236.
[105] Gerber, S., Rush, J., Stemman, O.,Kirschner, M., Gygi, S., Absolute quantification of proteins and phosphoproteins from cell lysates by tandem MS. Proceedings of the National Academy of Sciences 2003, 100, 12
[106] Bérczi, A. and Møller, I. M. (1987), Mg2+-ATPase activity in wheat root plasma membrane vesicles: Time-dependence and effect of sucrose and detergents. Physiologia Plantarum, 70: 583–589.